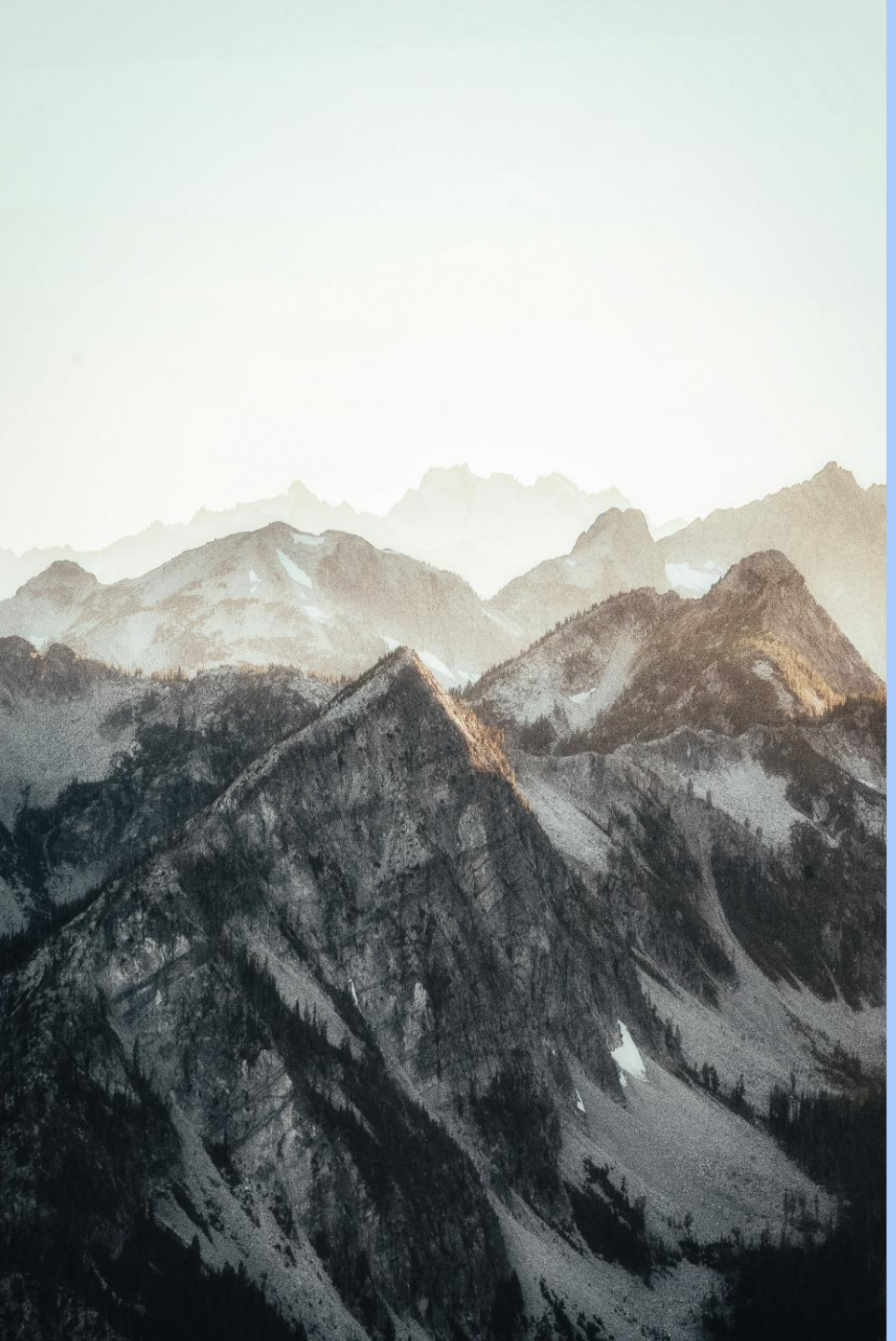

Disentangling

Axion-Like Particle

couplings to nucleons from a future

Galactic Supernova

DAVID ALONSO-GONZÁLEZ (he/him)
with D. Cerdeño, M. Cermeño & A.D. Perez

Based on [2412.19890]

SUPRISE 2025
(March 13th, Madrid)

Instituto de Física Teórica UAM-CSIC
Universidad Autónoma de Madrid

david.alonsogonzalez@uam.es

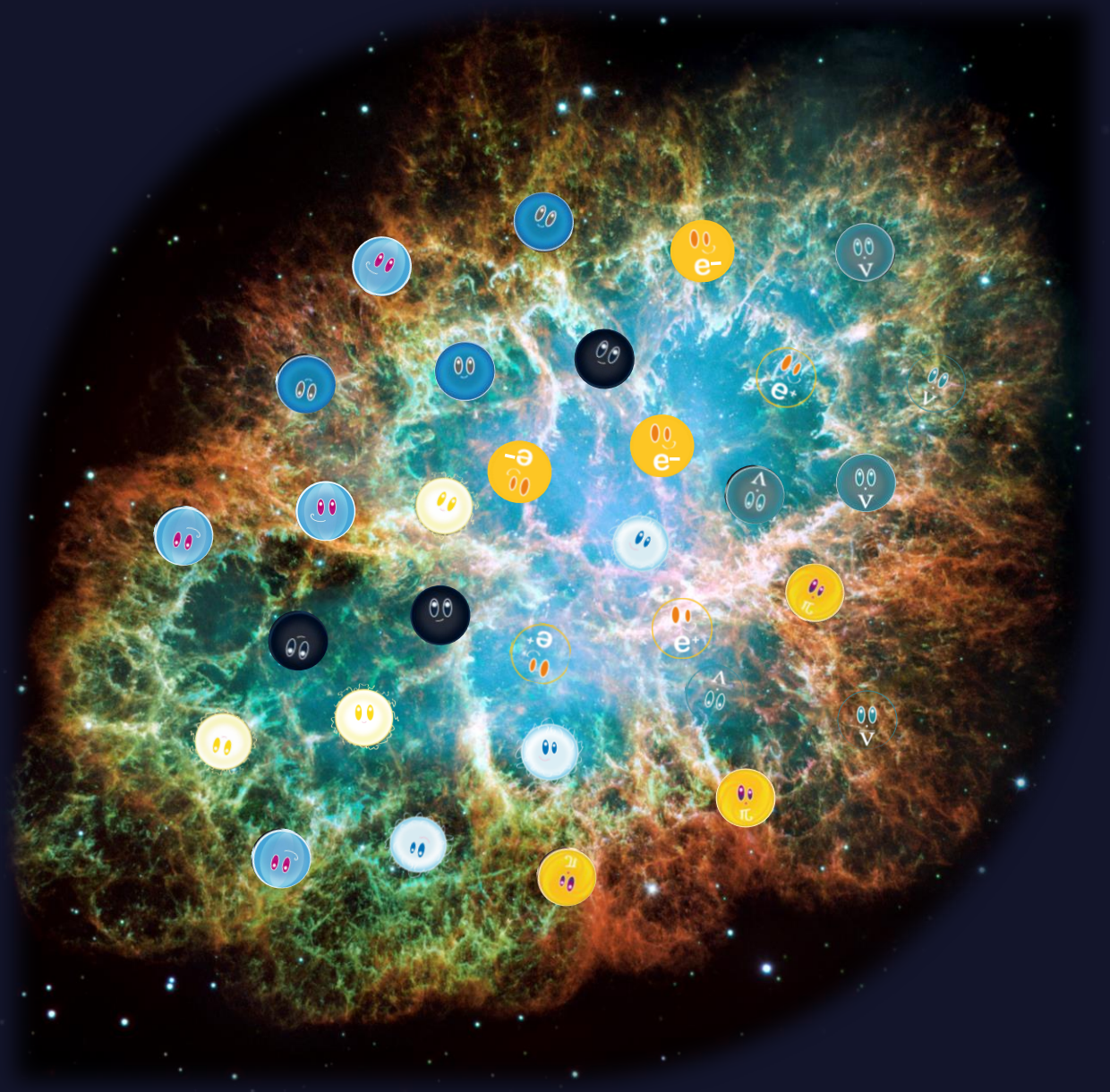

Crab Nebula [Hubble Space Telescope]
Particle Zoo from deviantart.com/physicsandmore

OUR INGREDIENTS

1. **Core collapse supernovae (SNe):** extremely hot and dense
2. **Galactic SNe:** very close to us
3. **Axion-Like Particles**

I hope you followed Andres's talk!

What happens at lower masses?

+ a strategy to disentangle ALP couplings to nucleons!

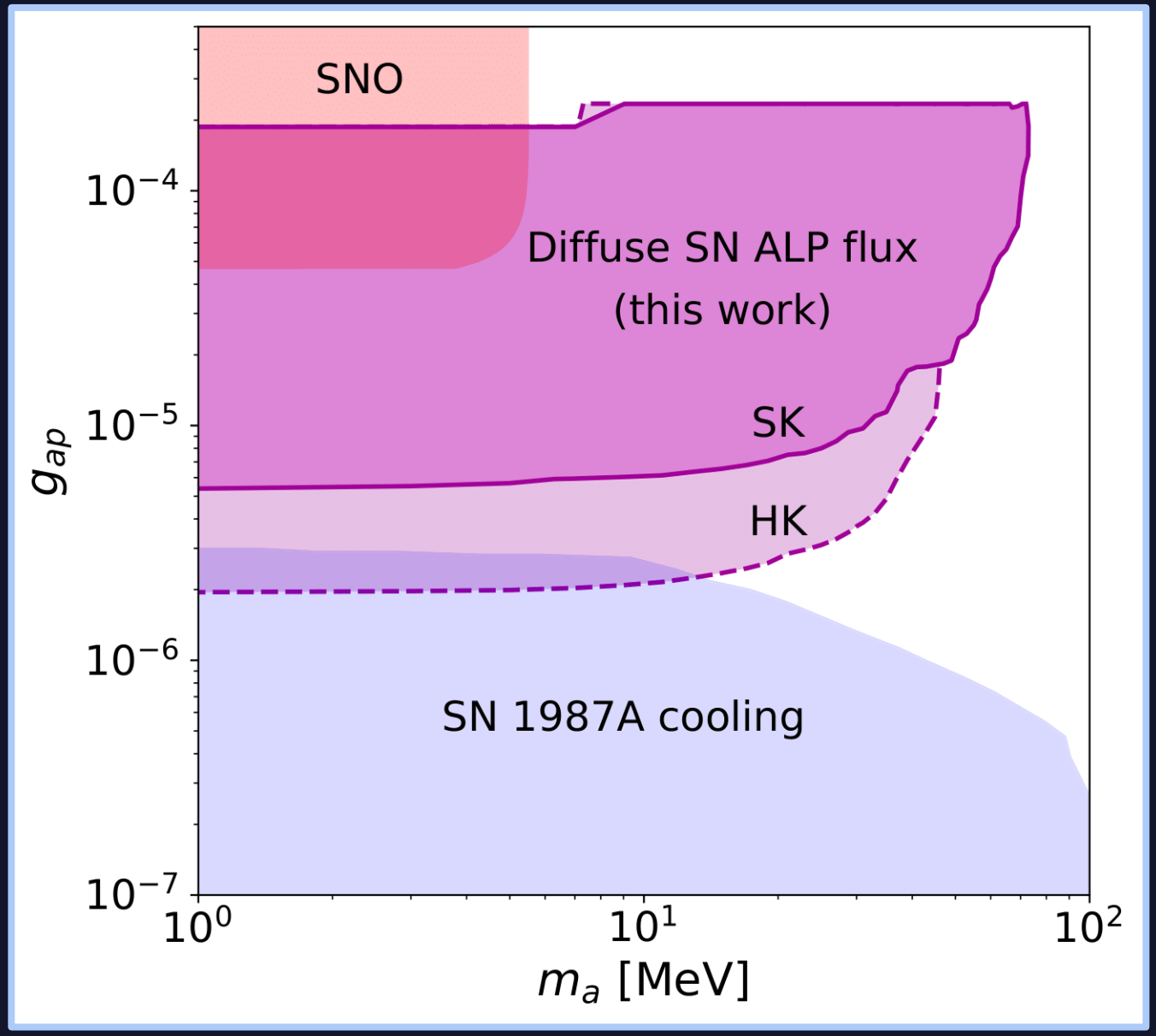

Alonso-González, Cerdeño, Cermeño, Perez [2412.19890]

OUTLINE

1. Motivation
2. ALP Production in SN
3. ALP Detection in Neutrino Water Cherenkov Detectors
4. Disentangling ALP-proton and ALP-neutron couplings
5. Conclusions

ALP-nucleon interaction

$$\mathcal{L}_{int} = g_a \frac{\partial_\mu a}{2\, m_N} \Big[C_{ap}\, \bar{p}\, \gamma^\mu \gamma_5\, p + C_{an}\, \bar{n}\, \gamma^\mu \gamma_5\, n + \frac{C_{a\pi N}}{f_\pi} \left(i\, \pi^+\, \bar{p}\, \gamma^\mu\, n - i\, \pi^-\, \bar{n}\, \gamma^\mu\, p \right) + C_{aN\Delta} \left(\bar{p}\, \Delta^+_\mu + \overline{\Delta^+_\mu}\, p + \bar{n}\, \Delta^0_\mu + \overline{\Delta^0_\mu}\, n \right) \Big]$$

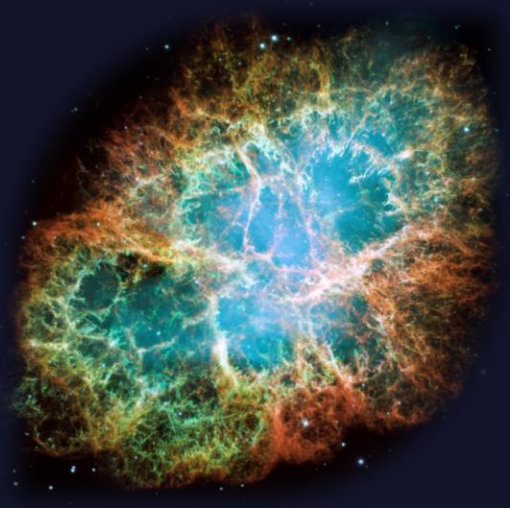

$\rho \sim 3 \cdot 10^{14}$ g/cm^3
$T \sim 30$ MeV

PARTICLES

a	ALP
p	Proton
n	Neutron
π^+, π^-	Pions
$\Delta^+_\mu, \overline{\Delta^+_\mu}, \Delta^0_\mu, \overline{\Delta^0_\mu}$	Delta Baryons

PARAMETERS

$g_a = m_N / f_a$	Dimensionless coupling constant
$m_N = 938$ MeV	Nucleon Mass
f_a	ALP scale
$f_\pi = 92.4$ MeV	Pion Decay Constant
C_{ap}, C_{an}	ALP-nucleon couplings
$C_{a\pi N} = (C_{ap} - C_{\mathrm{an}})/\sqrt{2} g_A$	ALP-pion-nucleon coupling
$C_{aN\Delta} = -\sqrt{3}/2 (C_{ap} - C_{\mathrm{an}})$	ALP-nucleon-delta coupling

Di Luzio et al. Phys. Rept. 870 (2020) 1
Chang, Choi PLB 316 (1993) 51

ALP production in SNe

$$\mathcal{L}_{int} = g_a \frac{\partial_\mu a}{2\, m_N} \left[C_{ap}\, \bar{p}\, \gamma^\mu \gamma_5\, p + C_{an}\, \bar{n}\, \gamma^\mu \gamma_5\, n + \frac{C_{a\pi N}}{f_\pi} \left(i\, \pi^+\, \bar{p}\, \gamma^\mu\, n - i\, \pi^-\, \bar{n}\, \gamma^\mu\, p \right) + C_{aN\Delta} \left(\bar{p}\, \Delta^+_\mu + \overline{\Delta^+_\mu}\, p + \bar{n}\, \Delta^0_\mu + \overline{\Delta^0_\mu}\, n \right) \right]$$

$NN \longrightarrow NNa$

Nucleon-nucleon Bremsstrahlung

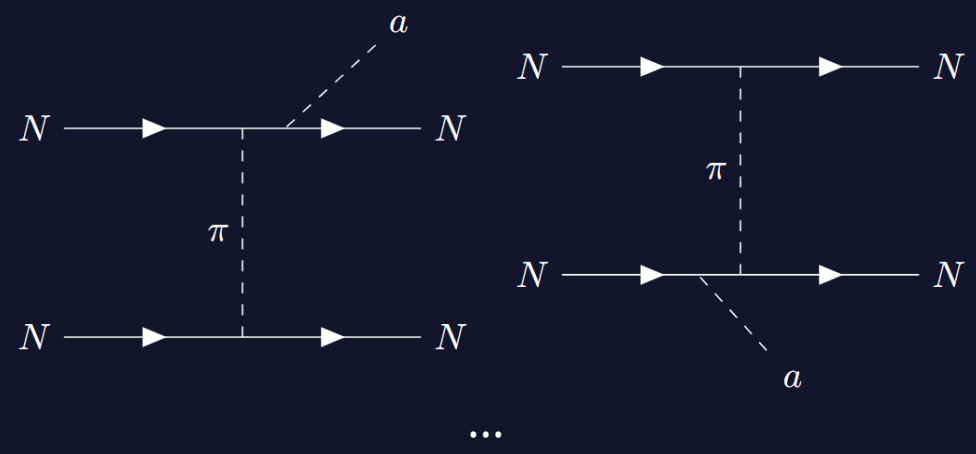

Carenza et al. JCAP 10 (2019) 016
Raffelt PR 198 (1990)

$\pi N \longrightarrow Na$

Pion-ALP Conversion

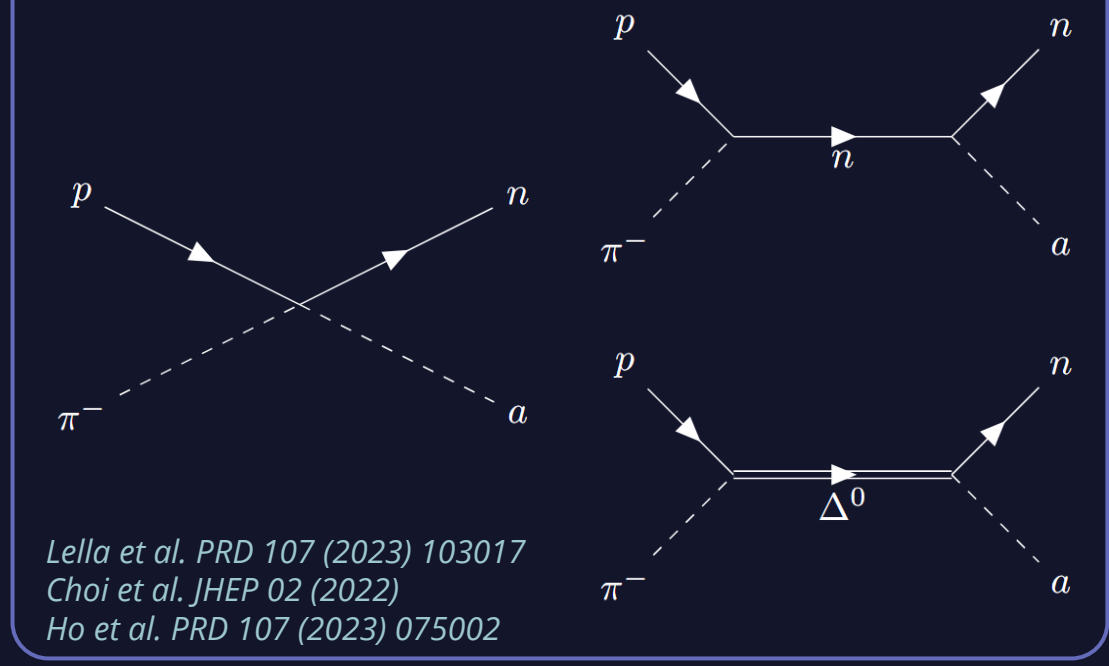

Lella et al. PRD 107 (2023) 103017
Choi et al. JHEP 02 (2022)
Ho et al. PRD 107 (2023) 075002

ALP production in a single SN

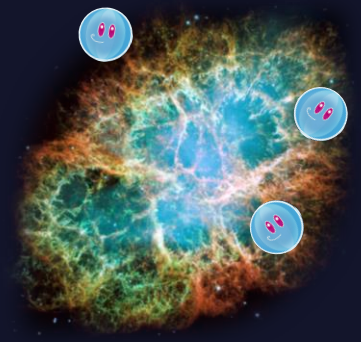

$$\frac{d^2 n_a}{dE_a dt} = \prod_i \int \frac{g_i \, d^3\vec{p_i}}{(2\pi)^3 2E_i} \prod_{j \neq a} \int \frac{d^3\vec{p_j'}}{(2\pi)^3 2E_j'} (2\pi)^4 \delta^4 \left(\sum_k p_k - \sum_{l \neq a} p_l' - p_a \right) \frac{|\vec{p_a}|}{4\pi^2} |\overline{M}|^2 \mathcal{F}(E_i, E_j')$$

incoming particles

outgoing particles (except ALP!)

four-momentum conservation

$p_i = (E_i, \vec{p_i})$: Four-momentum

E_i : Energy

$\vec{p_i}$: Three-momentum

$|\overline{M}|^2$: Squared spin-averaged matrix element

$$\mathcal{F}(E_i, E_j') = f_i(E_i)[1 - f_j(E_j')]$$

$$f_N = \frac{1}{e^{(E_N - \mu)/k_B T} + 1}$$: Fermi-Dirac distribution

$$f_\pi = \frac{1}{e^{(E_\pi - \mu)/k_B T} - 1}$$: Bose-Einstein distribution

ALP flux at Earth from a single SN

$$\frac{d\Phi_a}{dE_a^{Earth}} = \frac{1}{4\pi d_{SN}^2}\int_{t_{min}}^{t_{max}} dt \int_0^{\infty} \alpha(r)^{-1} 4\pi r^2 dr \left\langle e^{-\tau(E_a^*,t,r)} \right\rangle \frac{d^2 n_a}{dE_a^{loc} dt}\left(r, t, E_a^{loc}\right)$$

Lapse Function

Absorption Effects

$$\left\langle e^{-\tau(E_a^*,t,r)} \right\rangle = \frac{1}{2}\int_{-1}^{+1} d\mu\, e^{-\int_0^{\infty} ds \Gamma_a(E_a^*, \sqrt{r^2+s^2+2rs\mu})}$$

$$\Gamma_a(E_a^*, r) = \lambda_a^{-1}(E_a, r)\left[1 - e^{-\frac{E_a}{T(r)}}\right]$$

$$E_a^* = E_a \frac{\alpha(r)}{\alpha(\sqrt{r^2+s^2+2rs\mu})}$$

$$\alpha(r) = \sqrt{1 - 2\Delta\Phi(r)} \leq 1$$

$$\Delta\Phi(r) = G\int_r^{\infty} \frac{m_{enc}(r')}{r'^2} dr'$$

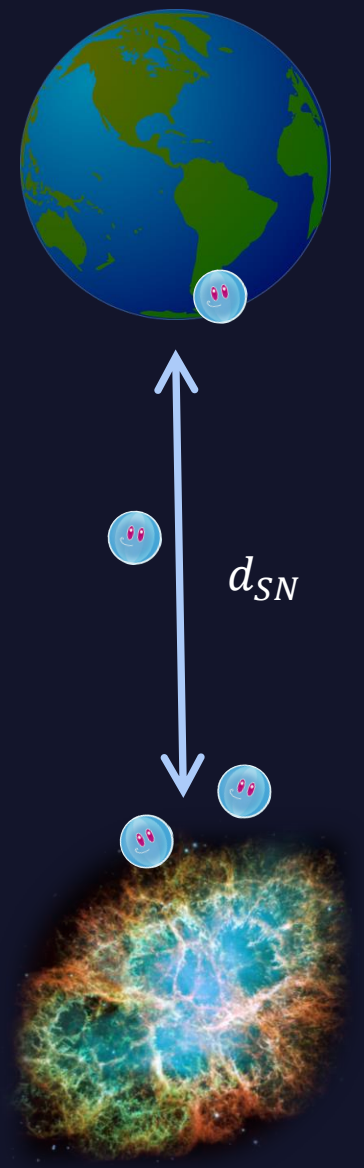

(not to scale!)

Lella et al. PRD 109 (2024) 023001
Carenza Eur. Phys. J. Plus 138 (2023) 836

ALP flux at Earth from a single SN

ALP flux reaching Earth from a SN at distance $d_{SN} = 1$ kpc for $m_a \leq 1$ MeV

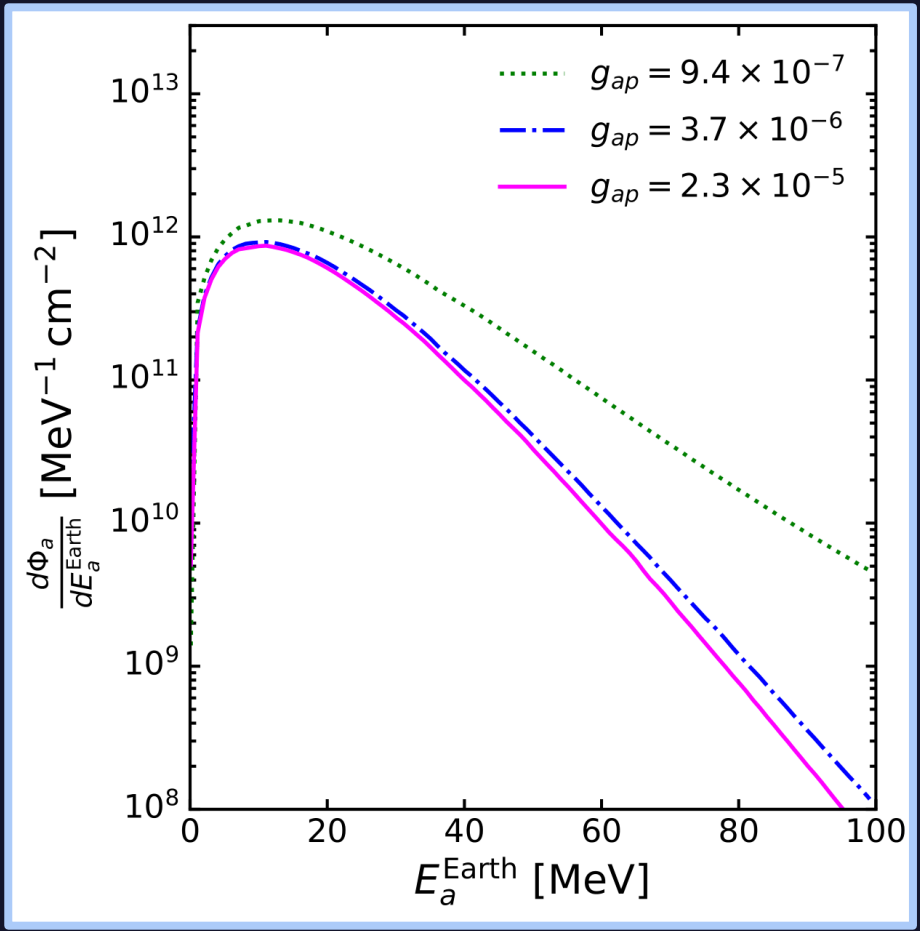

ALP detection in neutrino Cherenkov detectors

$$\mathcal{L}_{int} \ni g_{ap} \frac{\partial_\mu a}{2\, m_N} \bar{p}\, \gamma^\mu \gamma_5\, p \qquad \text{with } g_{ap} = g_a C_{ap}$$

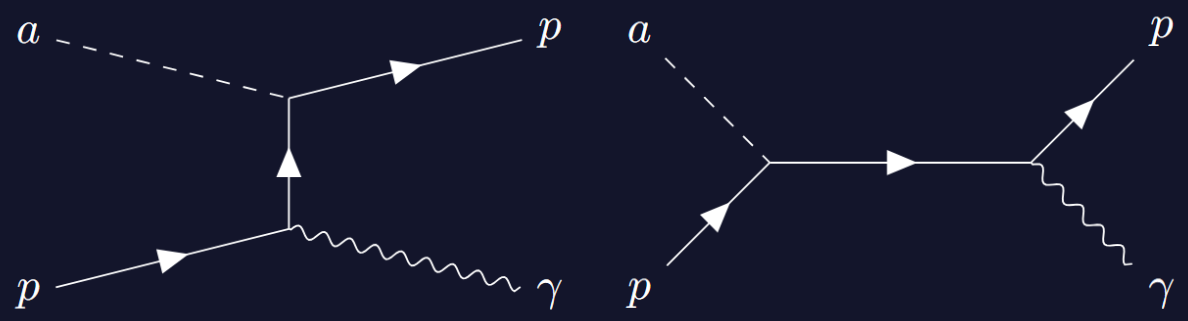

$$p + a \rightarrow p + \gamma$$

- Signature not been exploited before
- Rate **smaller** than oxygen de-excitation

$$a + {}^{16}O \longrightarrow {}^{16}O^{*} \longrightarrow {}^{16}O + \gamma$$

- However, released photon more energetic and almost **background free**

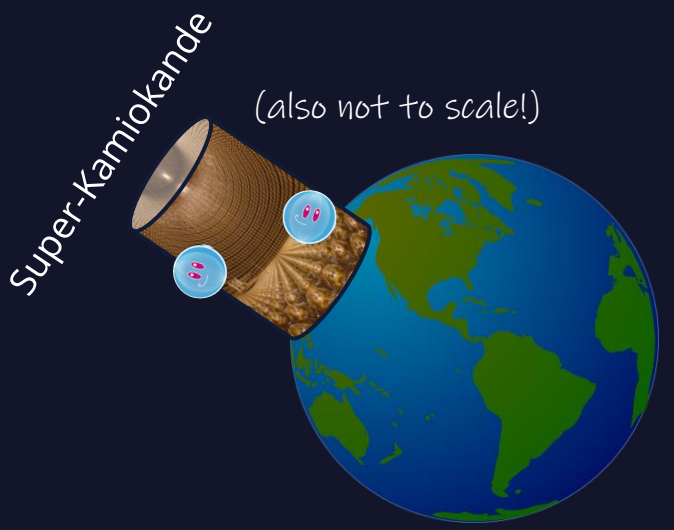

$$\frac{dN_\gamma}{dE_\gamma} = N_t \int_{E_a^{min}(E_\gamma)}^{E_a^{max}(E_\gamma)} dE_a^{Earth} \frac{d\Phi_a}{dE_a^{Earth}} \frac{d\sigma_{ap}}{dE_\gamma}$$

$$E_a^{max}(E_\gamma) \sim E_a^{min}(E_\gamma) \sim E_\gamma$$

ALP detection in Super-Kamiokande

ALP flux reaching Earth from a SN at distance $d_{SN} = 1$ kpc for $m_a \leq 1$ MeV

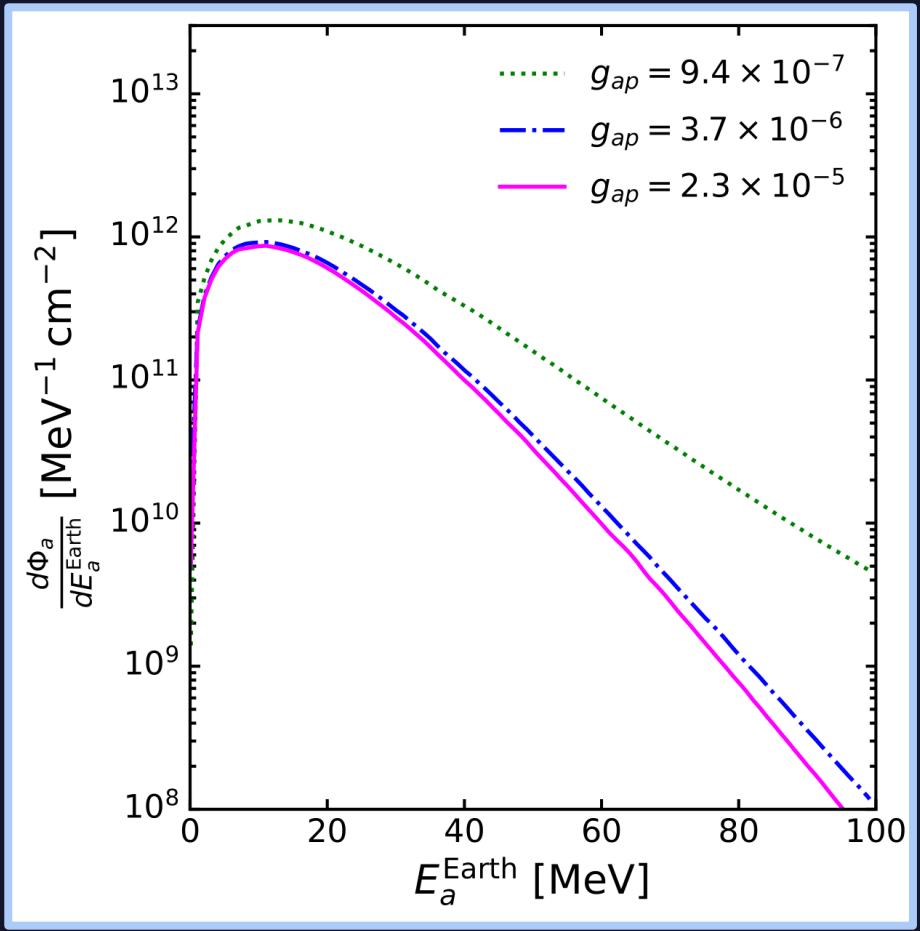

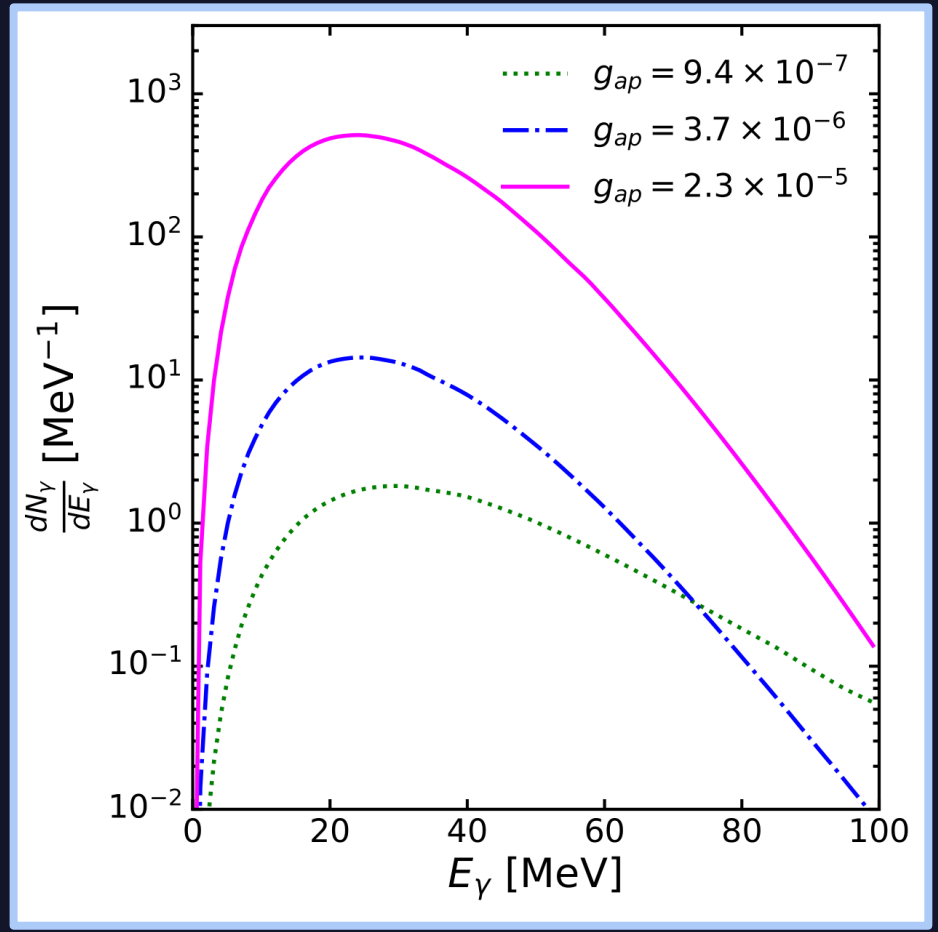

Differential photon spectrum produced by the ALP flux in Super-Kamiokande

ALP detection in Super-Kamiokande

In a future SN, ALPs would be **produced** at the **same time** as neutrinos.

However, due to their massive nature, they travel more slowly, leading to a **time delay** t_a between their arrival and the **first neutrino** event.

$$t_a \simeq \frac{d_{SN} m_a^2}{2E_a} \sim 2.01 \times 10^6 \text{ s} \left(\frac{d_{SN}}{1 \text{ kpc}}\right)\left(\frac{m_a}{0.1 \text{ MeV}}\right)^2 \left(\frac{16 \text{ MeV}}{E_a}\right)^2$$

In addition, since ALPs are produced with different energies, there will be a **time window** Δt_a between the first (most energetic) and the last measured ALPs.

$$\Delta t_a \simeq 1.93 \times 10^6 \text{s} \left(\frac{d_{SN}}{1 \text{ kpc}}\right)\left(\frac{m_a}{0.1 \text{ MeV}}\right)^2$$

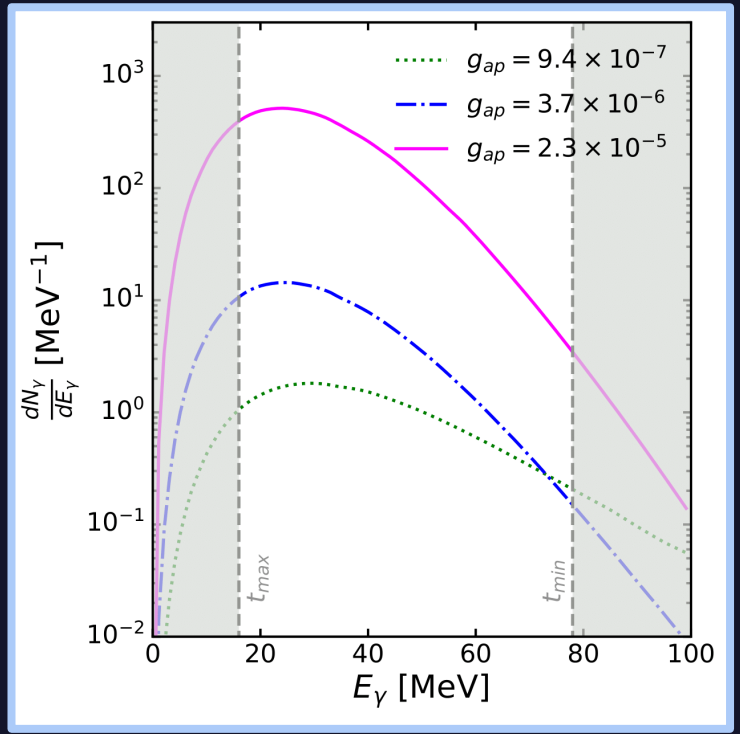

$E_a^{max} \sim E_a^{min} \sim E_\gamma$

$E_{rec} = [16,78]$ MeV

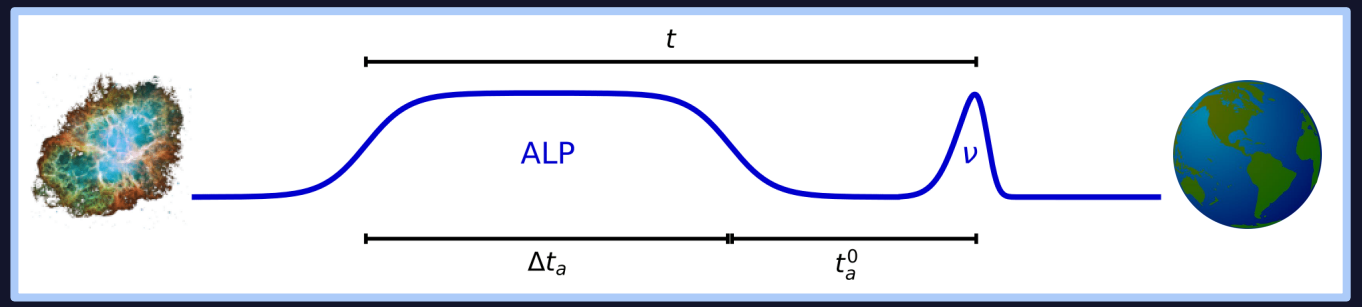

SIGNAL SIGNIFICANCE

$$Z(\Delta t_a) = \frac{N_\gamma(\Delta t_a)}{\sqrt{\bar{n}_{bkg} \Delta t_a}} \geq 2 \quad \text{(95\% C.L.)}$$

$$N_\gamma(\Delta t_a) \geq \max\left[2, 2\sqrt{\bar{n}_{bkg} \Delta t_a}\right]$$

ALP detection in Super-Kamiokande

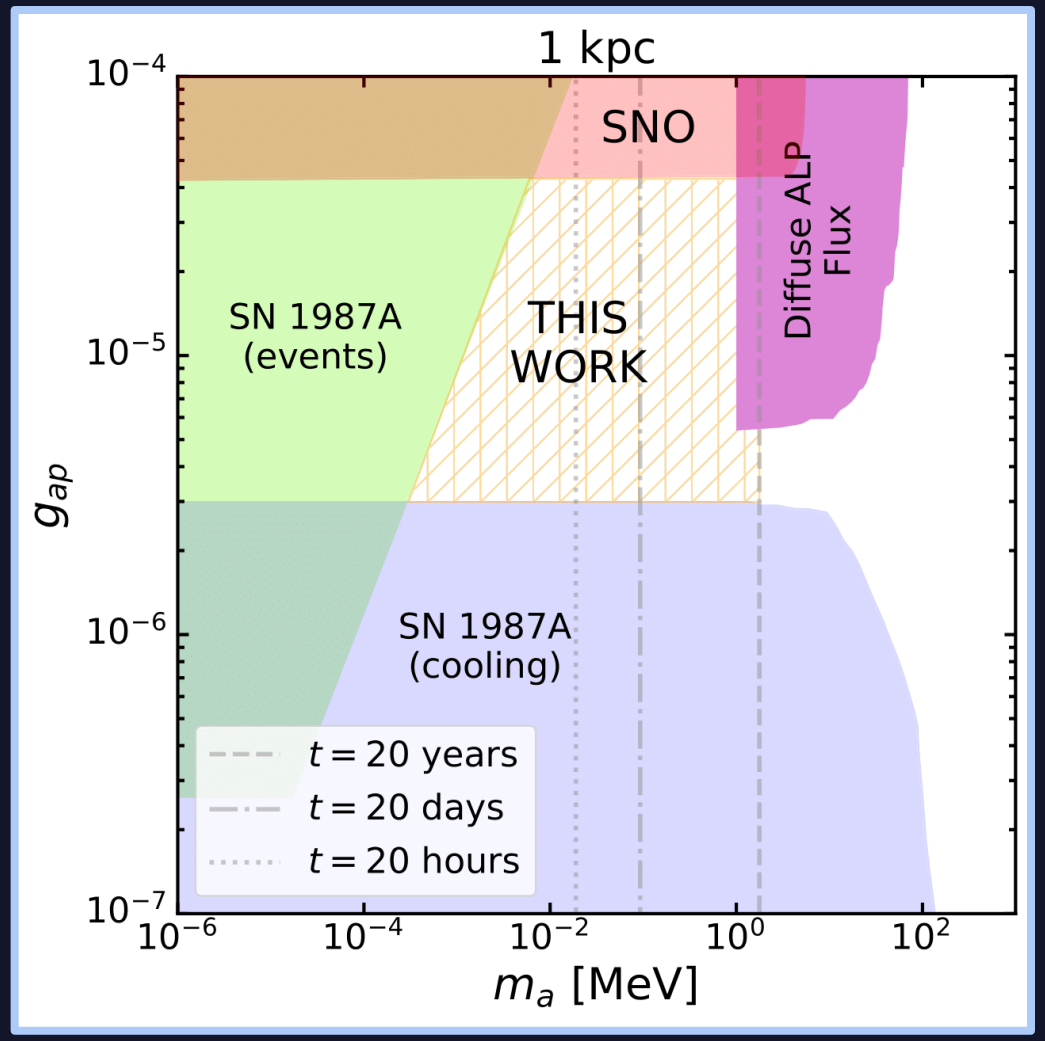

SNO

Bhusal, Houston, Li PRL 126 (2021) 091601

SN 1987A (cooling)

Lella, Carenza, Co', Lucente, Giannotti, Mirizzi, Rauscher PRD 109 (2024) 023001

SN 1987A (events)

Lella, Carenza, Co', Lucente, Giannotti, Mirizzi, Rauscher PRD 109 (2024) 023001

Diffuse ALP Flux

Alonso-González, Cermeño, Cerdeño, Perez [2412.09595]

ALP detection in Super-Kamiokande & Hyper-Kamiokande

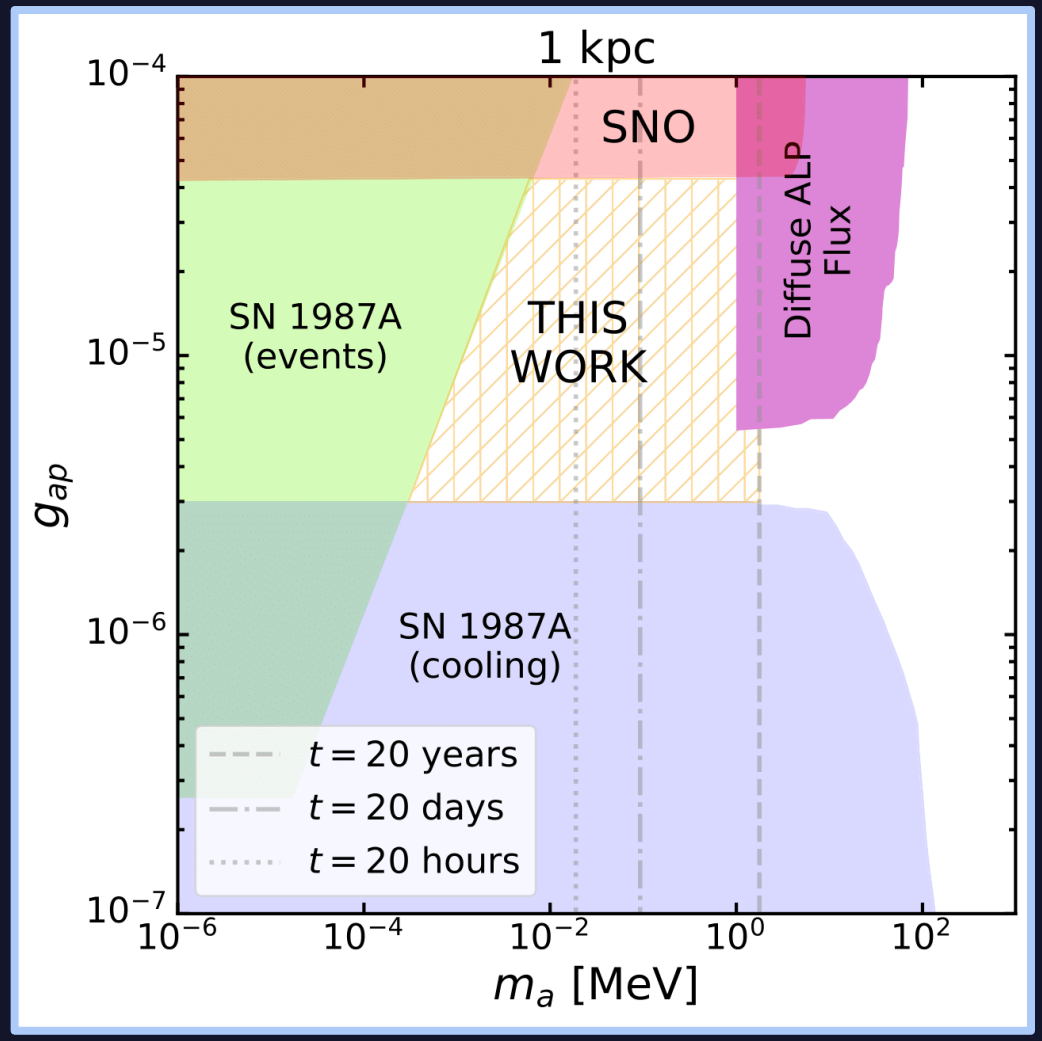

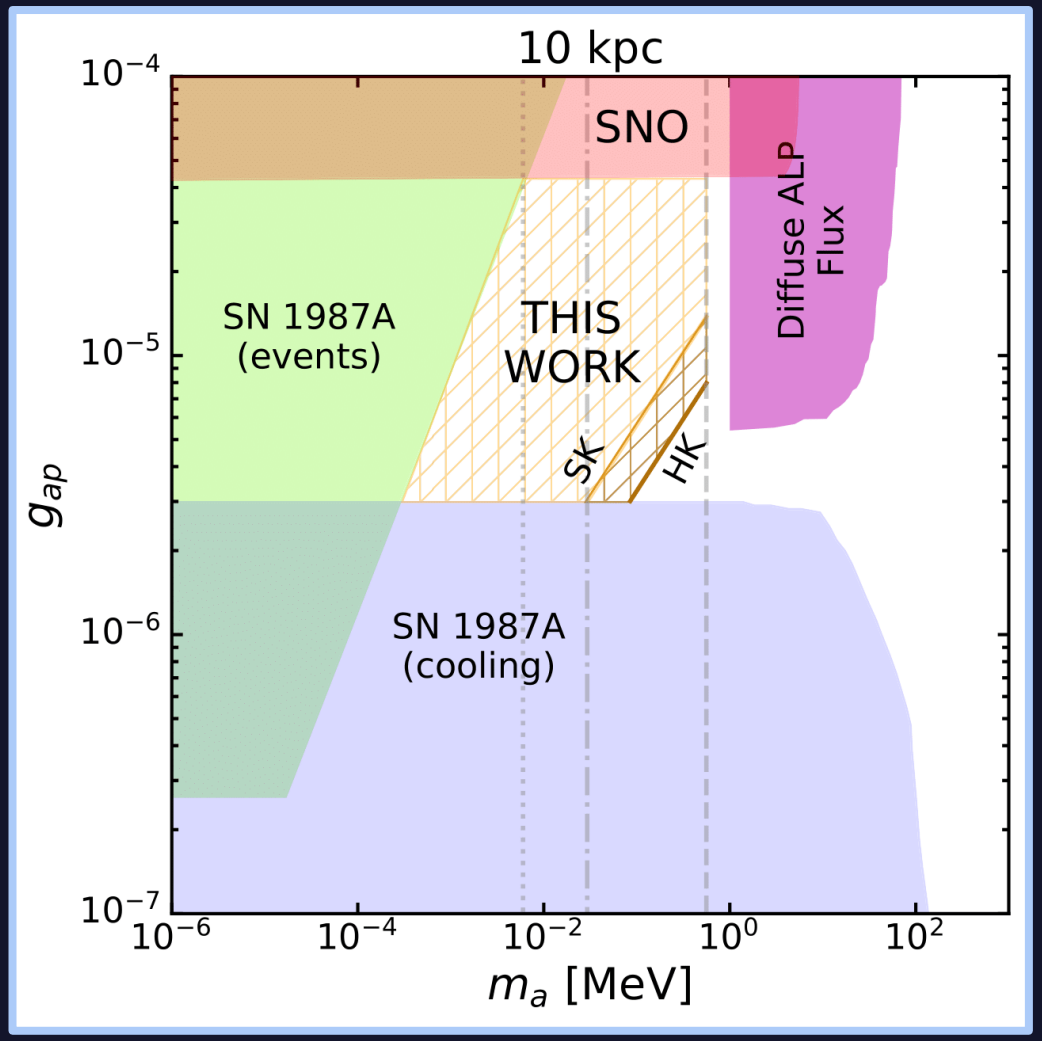

Disentangling **ALP** couplings to neutrons and protons

Our signature is only sensitive to **ALP-proton** coupling.

$$a + p \longrightarrow p + \gamma$$

Oxygen de-excitation depends on both the **ALP-proton** and **ALP-neutron** couplings.

$$a + {}^{16}O \longrightarrow {}^{16}O^{*} \longrightarrow {}^{16}O + \gamma$$

In a future SN observation, the comparison of both channels can be used to **measure the ratio** of both couplings.

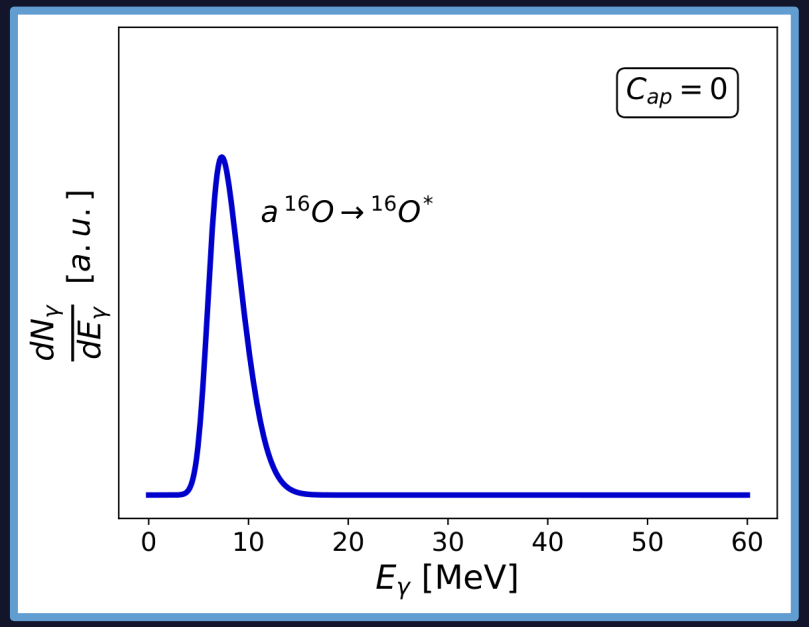

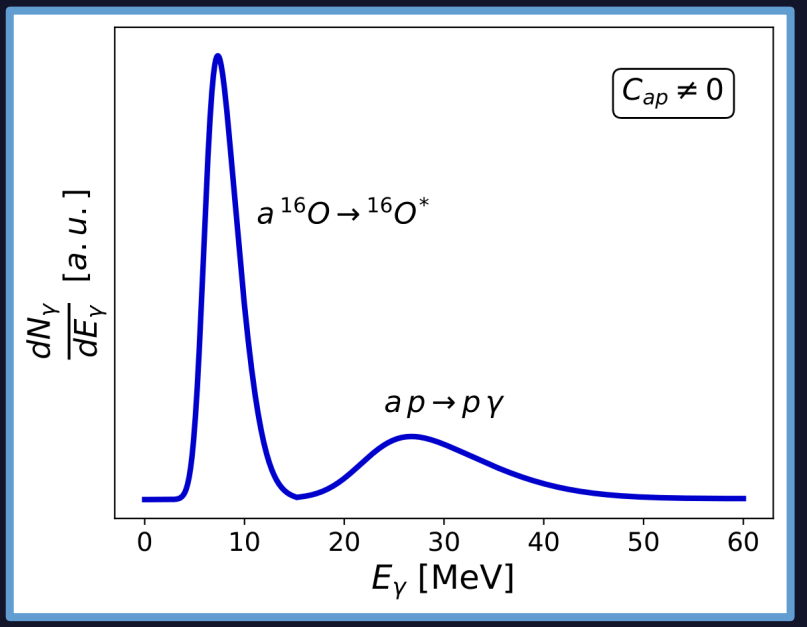

Disentangling **ALP** couplings to neutrons and protons

Our signature is only sensitive to **ALP-proton** coupling.

$$a + p \longrightarrow p + \gamma$$

Oxygen de-excitation depends on both the **ALP-proton** and **ALP-neutron** couplings.

$$a + {}^{16}O \longrightarrow {}^{16}O^{*} \longrightarrow {}^{16}O + \gamma$$

In a future SN observation, the comparison of both channels can be used to **measure the ratio** of both couplings.

This can be applied to supernovae up to ~ 100 kpc

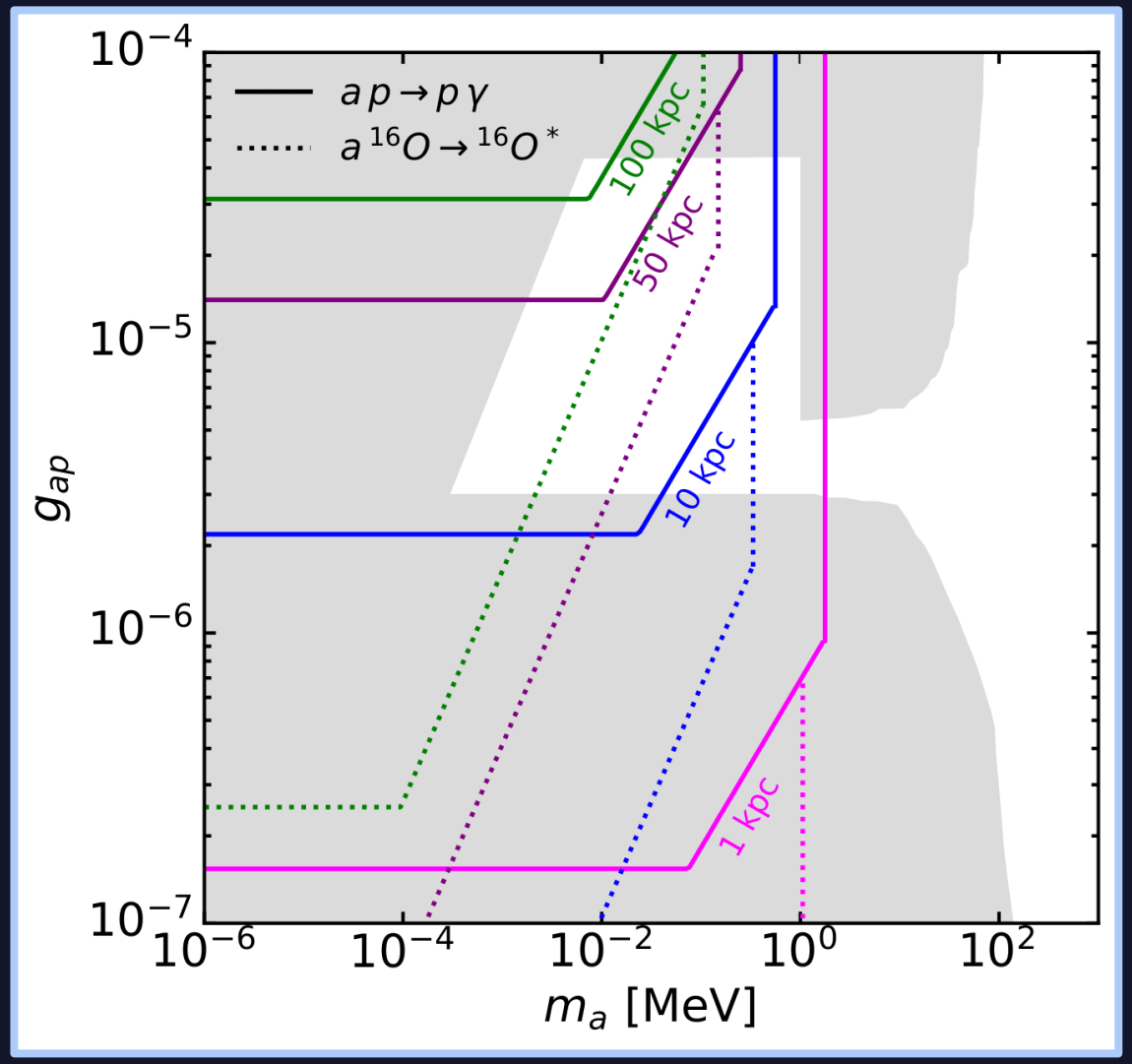

CONCLUSIONS

- If axion-like particles couple to protons, they can be produced in core-collapse supernovae and detected in neutrino water Cherenkov detectors via interactions with free protons

$$a + p \longrightarrow p + \gamma$$

- ALPs lighter than $m_a < 1$ MeV could be detected from single neighbouring supernova.
- Comparison of the signals from $a + p \longrightarrow p + \gamma$ and $a + {}^{16}O \longrightarrow {}^{16}O^*$ can be used to disentangle the ALP coupling to neutrons and protons.
- This could be done for supernovae as distant as ~ 100 kpc.

Thanks for your attention!

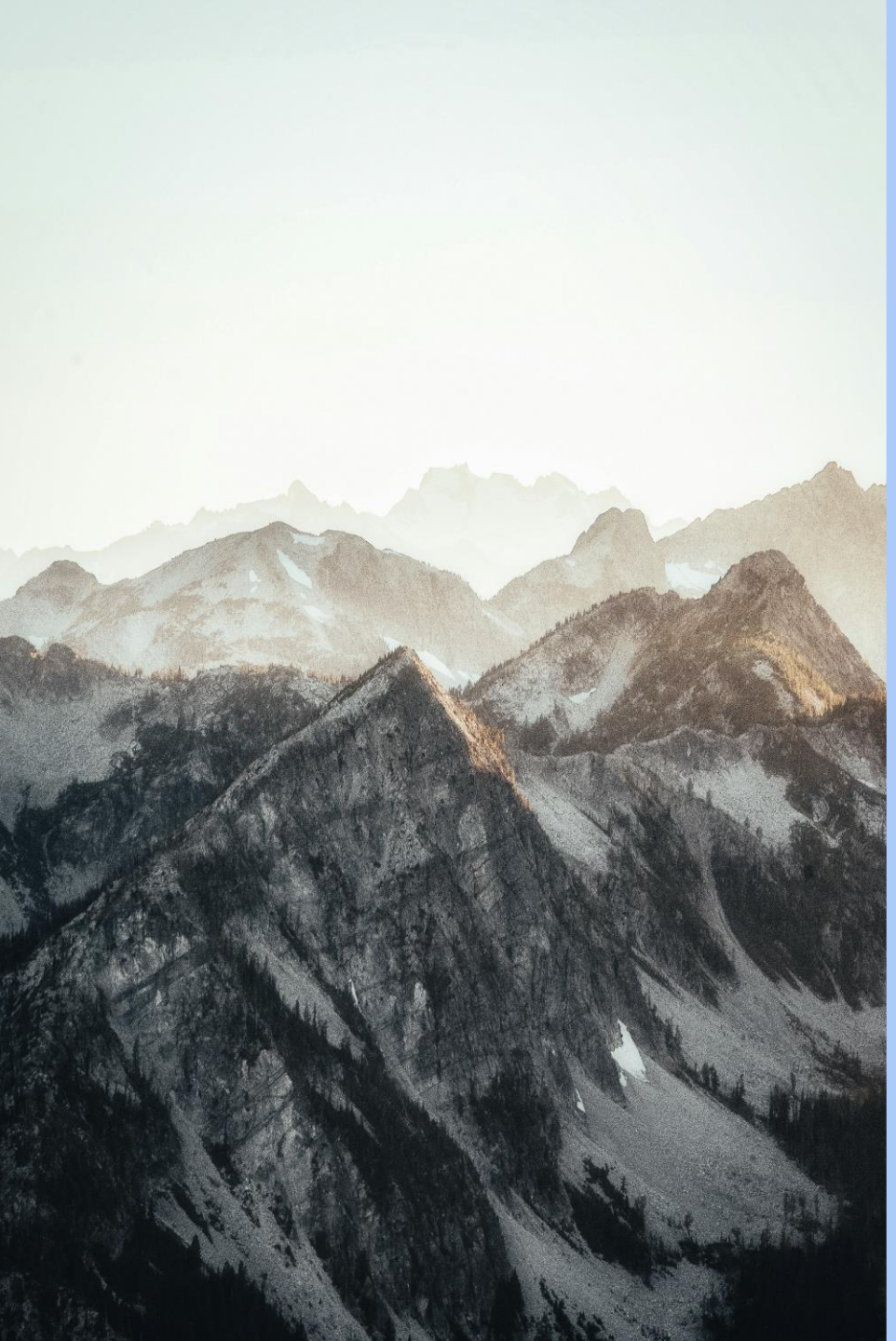

Backup Slides

SN Evolution

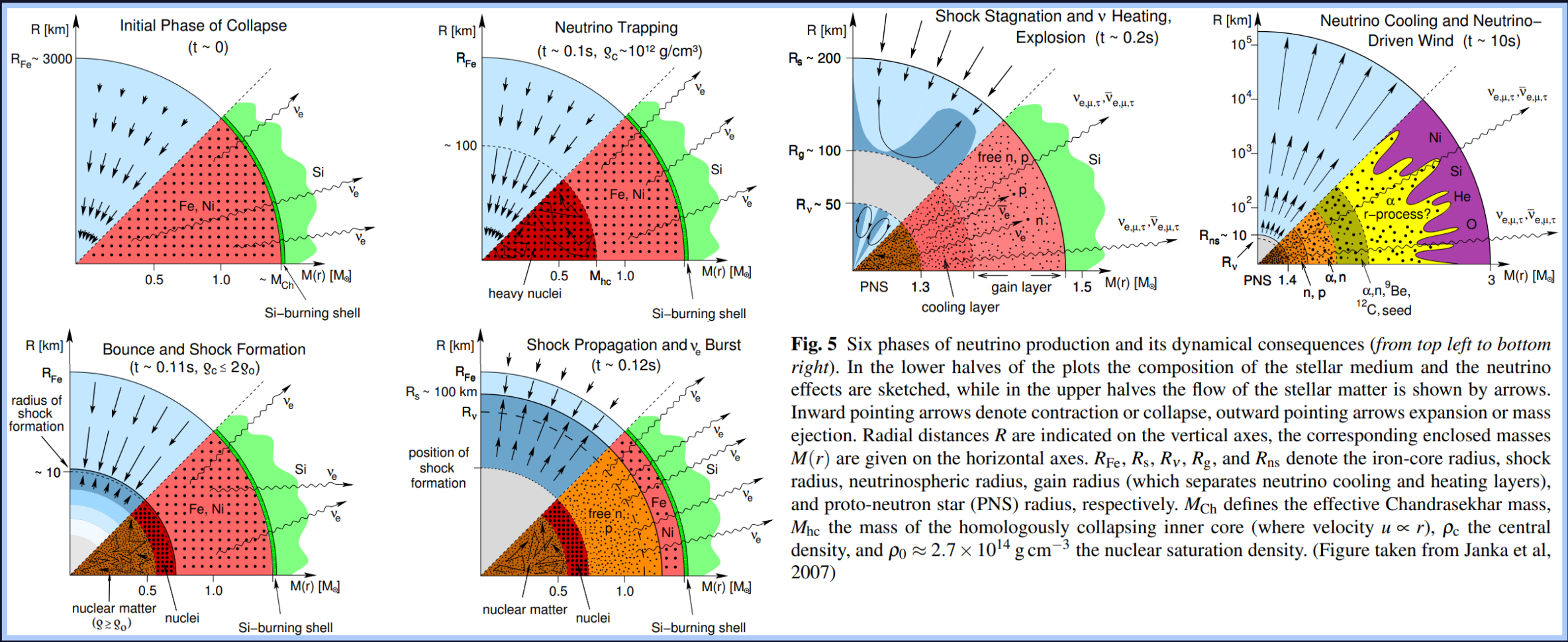

Fig. 5 Six phases of neutrino production and its dynamical consequences (*from top left to bottom right*). In the lower halves of the plots the composition of the stellar medium and the neutrino effects are sketched, while in the upper halves the flow of the stellar matter is shown by arrows. Inward pointing arrows denote contraction or collapse, outward pointing arrows expansion or mass ejection. Radial distances R are indicated on the vertical axes, the corresponding enclosed masses $M(r)$ are given on the horizontal axes. $R_{\rm Fe}$, $R_{\rm s}$, R_{ν}, $R_{\rm g}$, and $R_{\rm ns}$ denote the iron-core radius, shock radius, neutrinospheric radius, gain radius (which separates neutrino cooling and heating layers), and proto-neutron star (PNS) radius, respectively. $M_{\rm Ch}$ defines the effective Chandrasekhar mass, $M_{\rm hc}$ the mass of the homologously collapsing inner core (where velocity $u \propto r$), $\rho_{\rm c}$ the central density, and $\rho_0 \approx 2.7 \times 10^{14}\,{\rm g\,cm^{-3}}$ the nuclear saturation density. (Figure taken from Janka et al, 2007)

Janka [1702.08713]

SN Profile for $t = 1$ s post-bounce

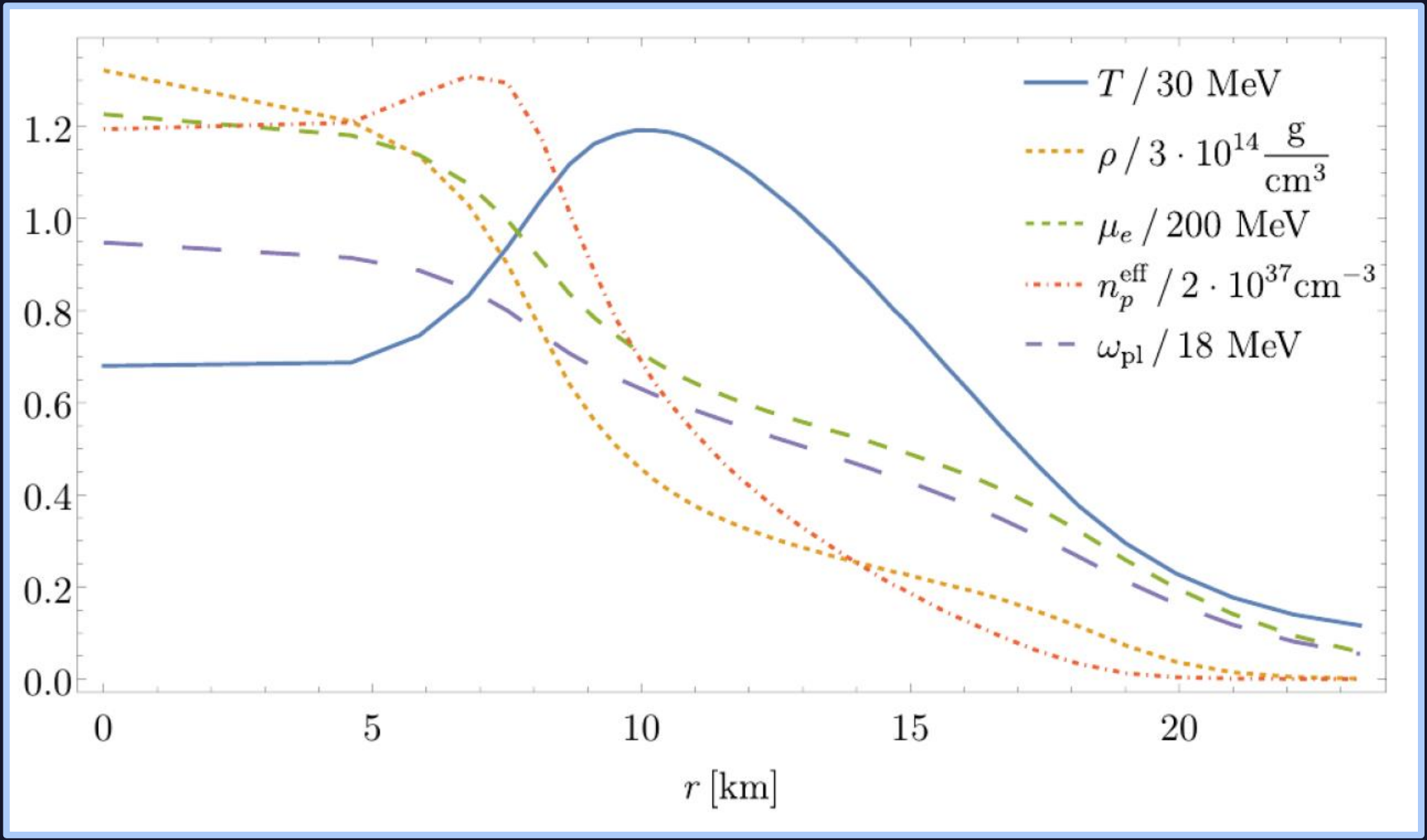

Ferreira, Marsh, Müller, JCAP 11 (2022) 057

Effect of **ALP**s on the profiles

$t = 1$ s post-bounce

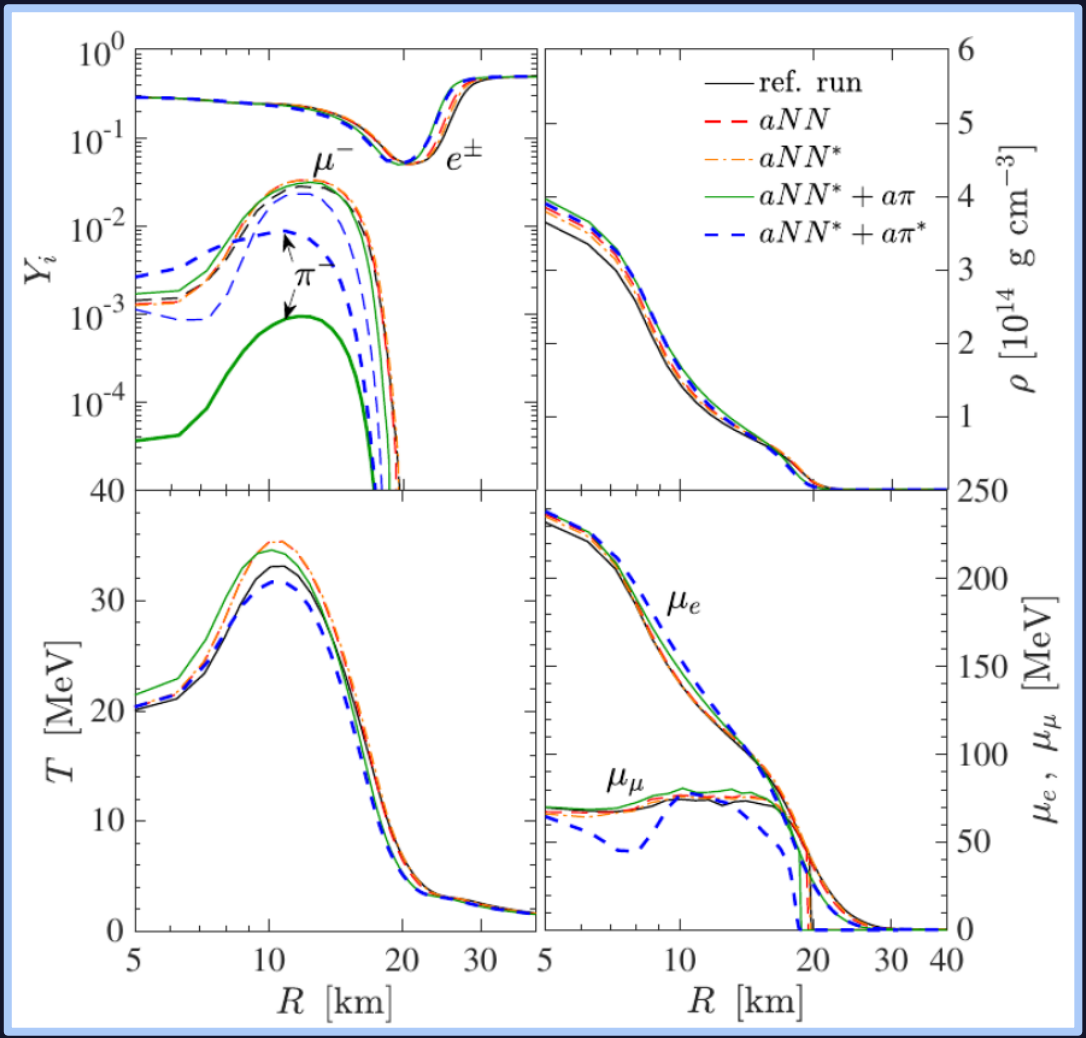

$t = 7$ s post-bounce

Fischer et al., PRD 104 (2021) 103012

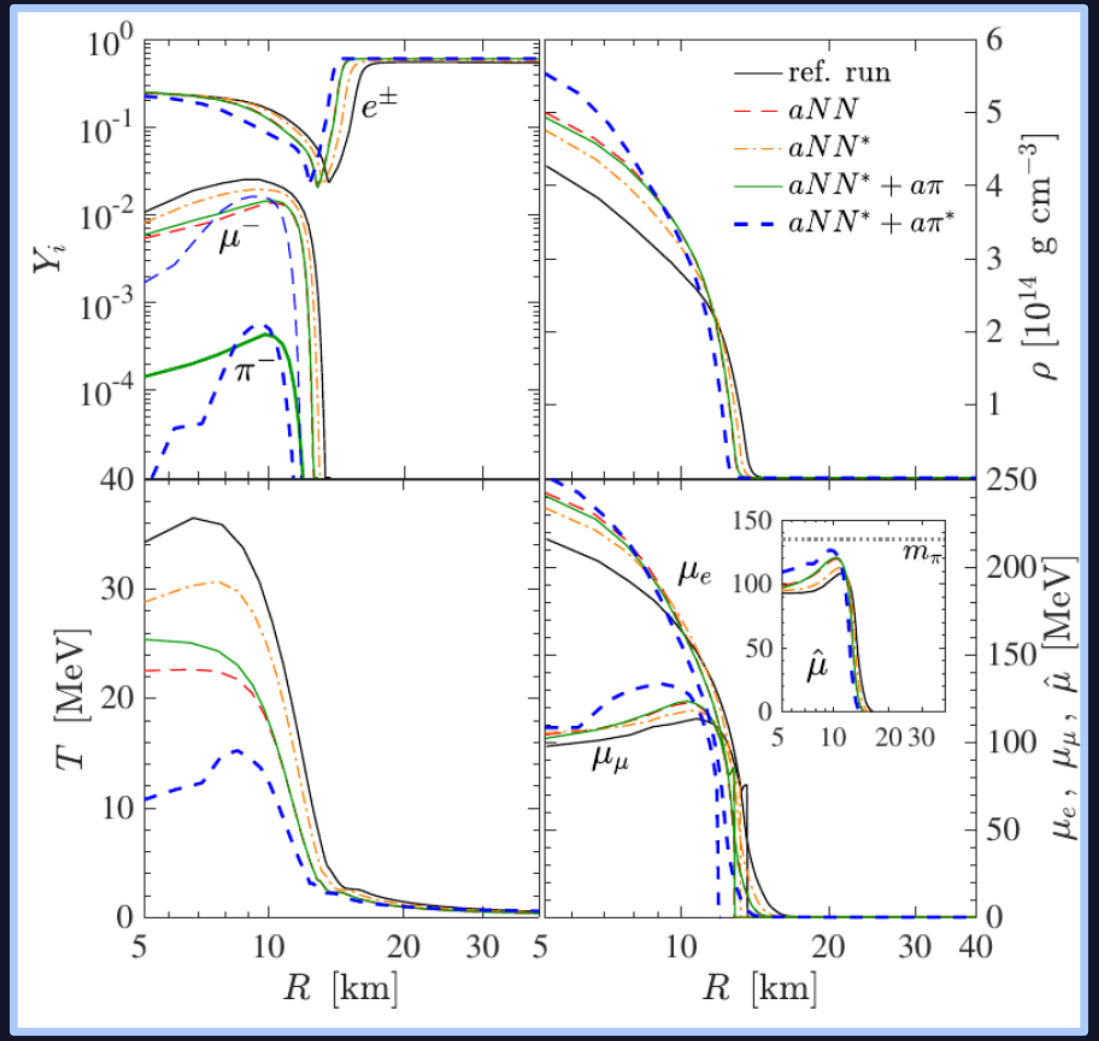

ALP production in SN: **Bremsstrahlung**

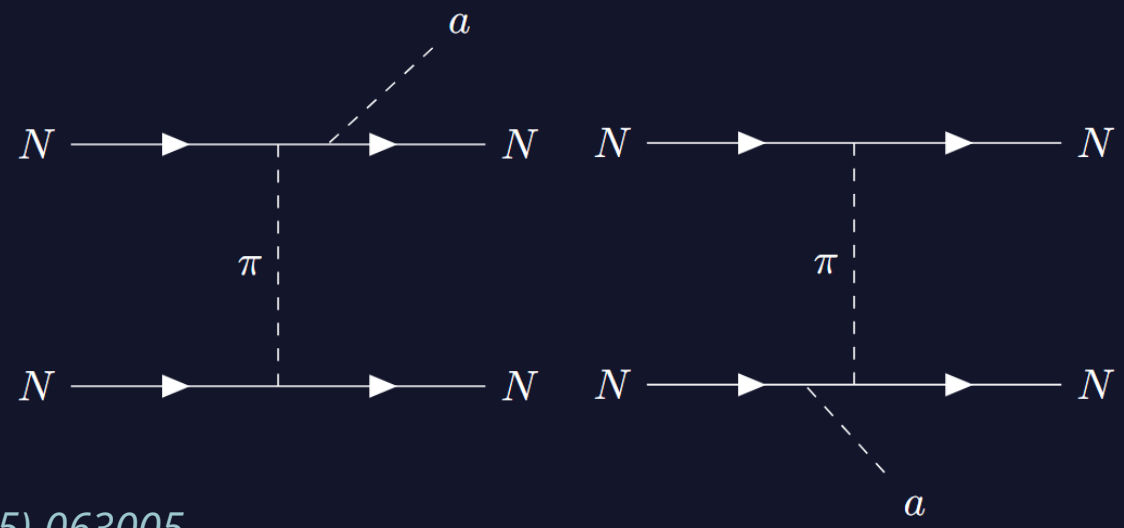

Gianotti, Nesti, PRD 72 (2005) 063005

$$\left(\frac{d^2 n_a}{dE_a dt}\right)_{NN} = \frac{g_a^2}{16\pi^2}\frac{n_B}{m_N^2}(E_a^2 - m_a^2)^{\frac{3}{2}} e^{-\frac{E_a}{T}} S_\sigma(E_a)\Theta(E_a - m_a)$$

$S_\sigma(E_a) = \frac{\Gamma_\sigma}{E_a^2 + g^2\Gamma_\sigma^2} s\left(\frac{E_a}{T}\right)$: Nucleon structure function

$s\left(\frac{E_a}{T}\right)$: Dimensionless nucleon function

$\Gamma_\sigma = 4\pi^{-1.5}\left(\frac{g_A}{2f_\pi}\right)^4 T^{0.5} m_N^{0.5}\rho$: Nucleon spin fluctuation rate

ALP production in SN: **pion-axion conversion**

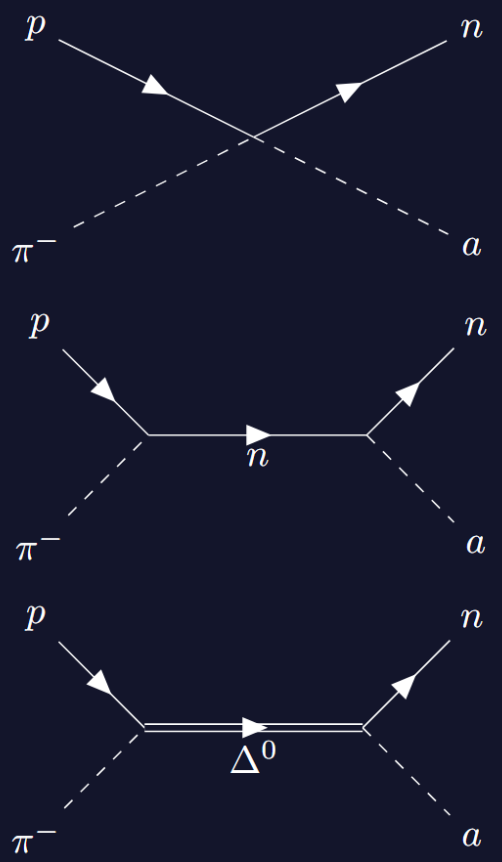

Carenza et al., PRL 126 (2021) 071102

$$\left(\frac{d^2 n_a}{dE_a dt}\right)_{N\pi} = \frac{g_a^2 T^{1.5}}{2^{1.5}\pi^5 m_N^{0.5}} \left(\frac{g_A}{2f_\pi}\right)^2 (E_a^2 - m_a^2)^{\frac{1}{2}}$$

$$\times C_a^{p\pi-} \frac{\Theta(E_a - \max(m_a, m_\pi))}{\exp(x_a - y_\pi - \widehat{\mu_\pi}) - 1} (E_a^2 - m_\pi^2)^{\frac{1}{2}} \frac{E_a^2}{E_a^2 + \Gamma^2}$$

$$\times \int_0^\infty dy\, y^2 \frac{1}{\exp\left(y^2 - \widehat{\mu_p}\right) + 1} \frac{1}{\exp(-y^2 + \widehat{\mu_n}) + 1}$$

$$C_a^{p\pi^-} = \frac{m_N^2}{g_A^2} \beta_a^2 \mathcal{G}_a(|\boldsymbol{p}_\pi|)$$

ALP production in SNe from $\gamma\, p \rightarrow a\, p$

$$\mathcal{L}_{int} = g_a \frac{\partial_\mu a}{2\, m_N} \left[C_{ap}\, \bar{p}\, \gamma^\mu \gamma_5\, p + C_{an}\, \bar{n}\, \gamma^\mu \gamma_5\, n + \frac{C_{a\pi N}}{f_\pi} \left(i\, \pi^+\, \bar{p}\, \gamma^\mu\, n - i\, \pi^-\, \bar{n}\, \gamma^\mu\, p \right) + C_{aN\Delta} \left(\bar{p}\, \Delta^+_\mu + \overline{\Delta^+_\mu}\, p + \bar{n}\, \Delta^0_\mu + \overline{\Delta^0_\mu}\, n \right) \right]$$

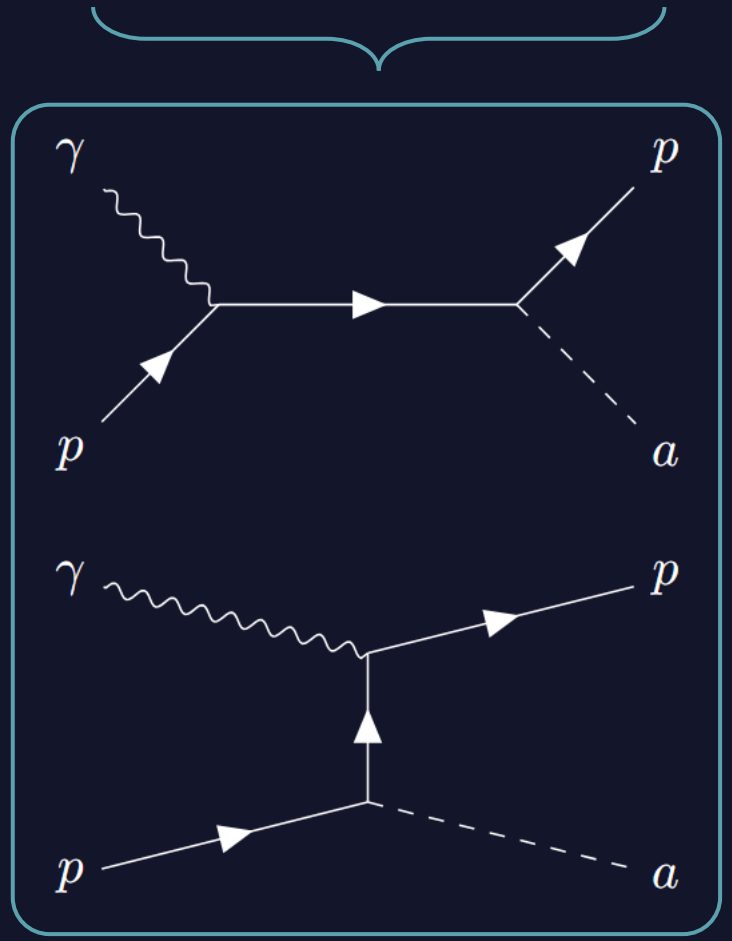

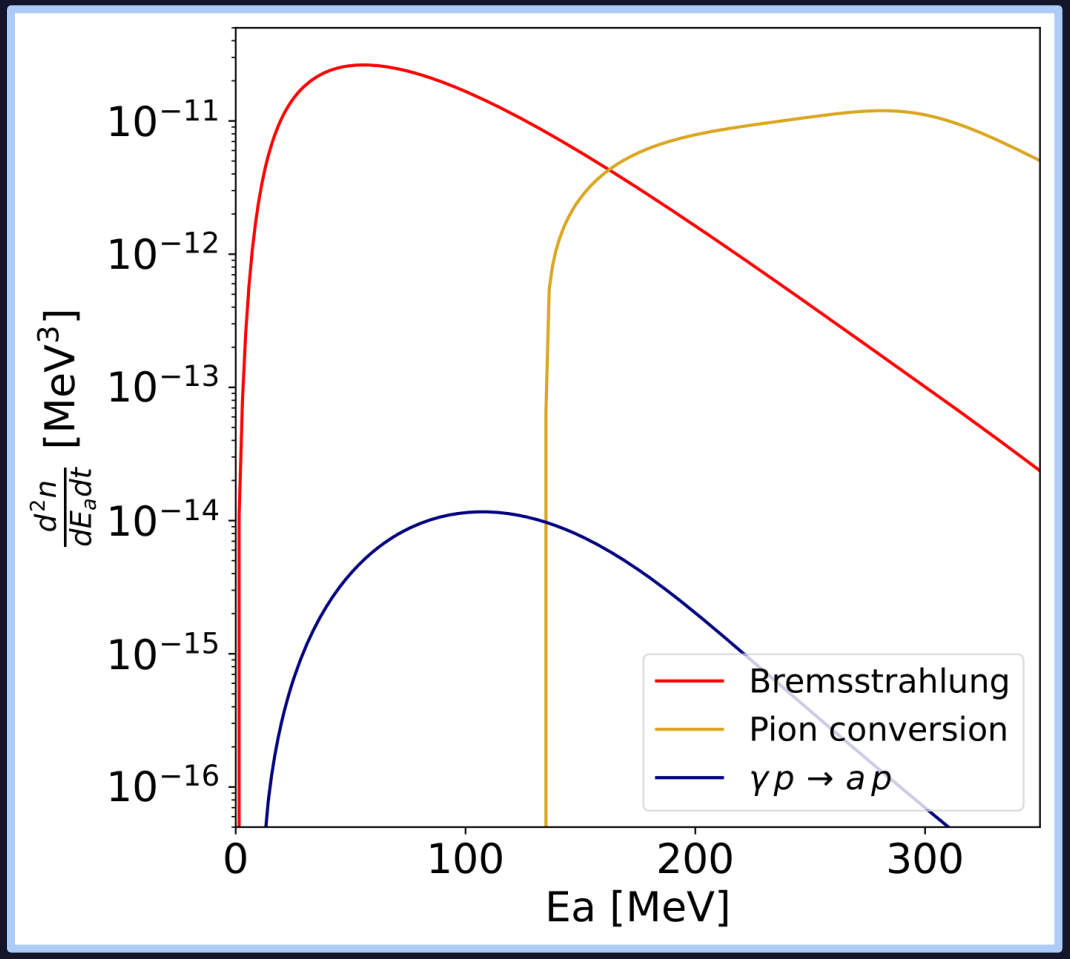

Lapse Function

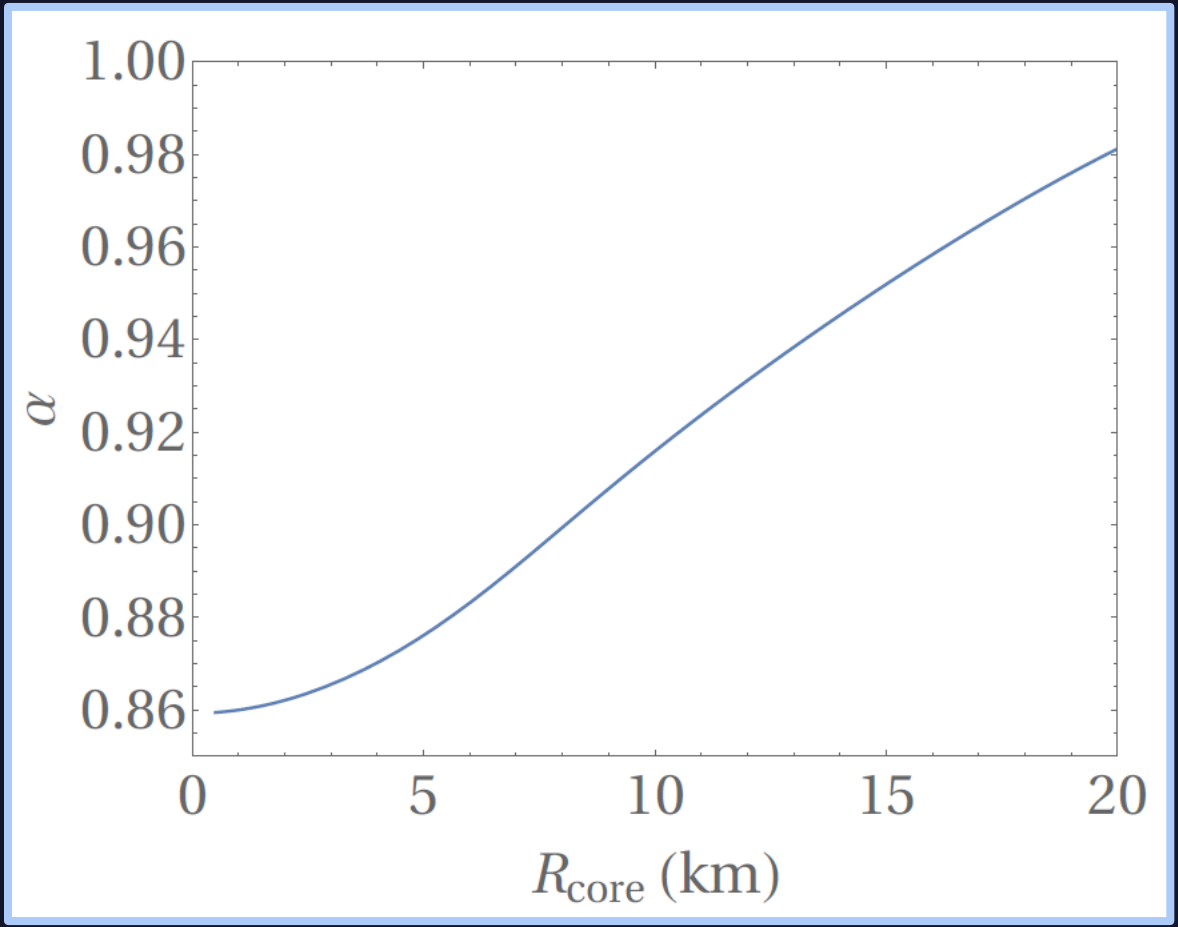

Lapse function encodes effects due to the proto-NS gravitational potential $\Phi(r)$ evaluated locally in the proto-NS interior

$$\alpha(r) = \sqrt{1 - 2\Delta\Phi(r)} \leq 1$$

$$\Delta\Phi(r) = G \int_r^{\infty} \frac{m_{enc}(r')}{r'^2} dr'$$

ALP detection in neutrino Cherenkov detectors

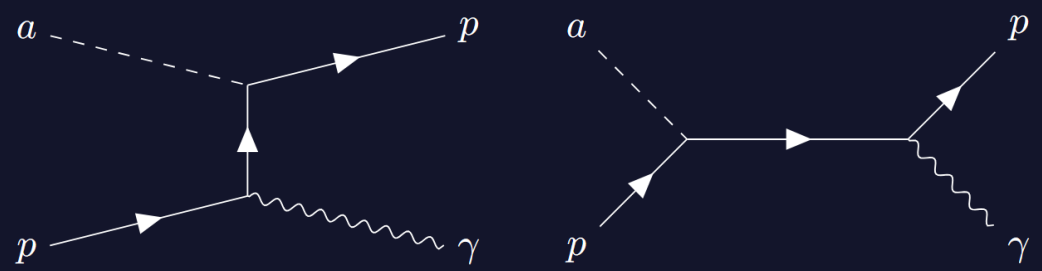

$$\frac{d\sigma_{ap}}{dE_\gamma} = \frac{1}{32\pi}\int_{-1}^{1} \frac{|\overline{M}|^2_{ap}}{|\vec{p}_a|^2 m_p}\,\delta(\cos\theta - \cos\theta_0)\,d\cos\theta$$

$$|\overline{M}|^2_{ap} = \frac{e^2 g_{ap}^2}{E_\gamma^2 m_p (2E_a m_p + m_a^2)^2}\Big[4m_p^3(E_a - E_\gamma)^2(2E_a E_\gamma + m_a^2)$$

$$+4m_a^2 m_p^2(E_a - E_\gamma)(E_\gamma(E_a - E_\gamma) + m_a^2)$$

$$+m_a^4 m_p(2E_a E_\gamma + m_a^2) + E_\gamma m_a^6\Big]$$

$$\cos\theta_0 = \frac{E_\gamma(m_p + E_a) - 2m_p E_a - m_a^2}{2E_\gamma\sqrt{E_a^2 - m_a^2}}$$

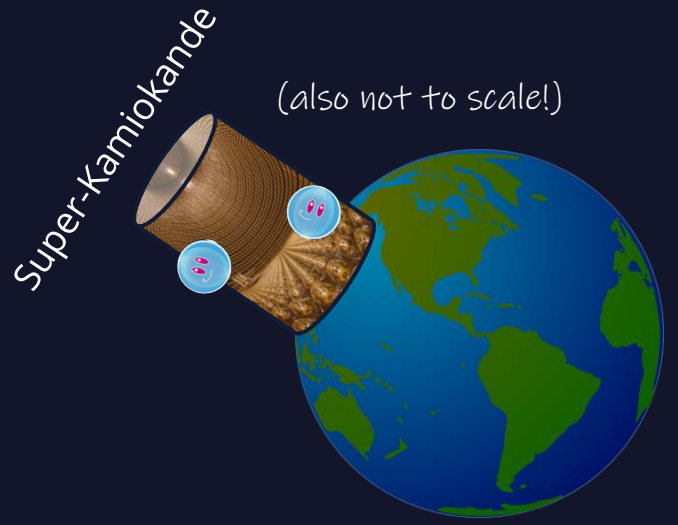

$$\frac{dN_\gamma}{dE_\gamma} = N_t \int_{E_a^{min}(E_\gamma)}^{E_a^{max}(E_\gamma)} dE_a^{Earth}\,\frac{d\Phi_a}{dE_a^{Earth}}\,\frac{d\sigma_{ap}}{dE_\gamma}$$

$$E_\gamma^{min} = \frac{m_a^2 + 2E_a m_p}{2(m_p + E_a) - 2\sqrt{E_a^2 - m_a^2}}$$

$$E_\gamma^{max} = \frac{m_a^2 + 2E_a m_p}{2(m_p + E_a) + 2\sqrt{E_a^2 - m_a^2}}$$

$$E_a^{max}(E_\gamma) \sim E_a^{min}(E_\gamma) \sim E_\gamma$$

Super-Kamiokande Background

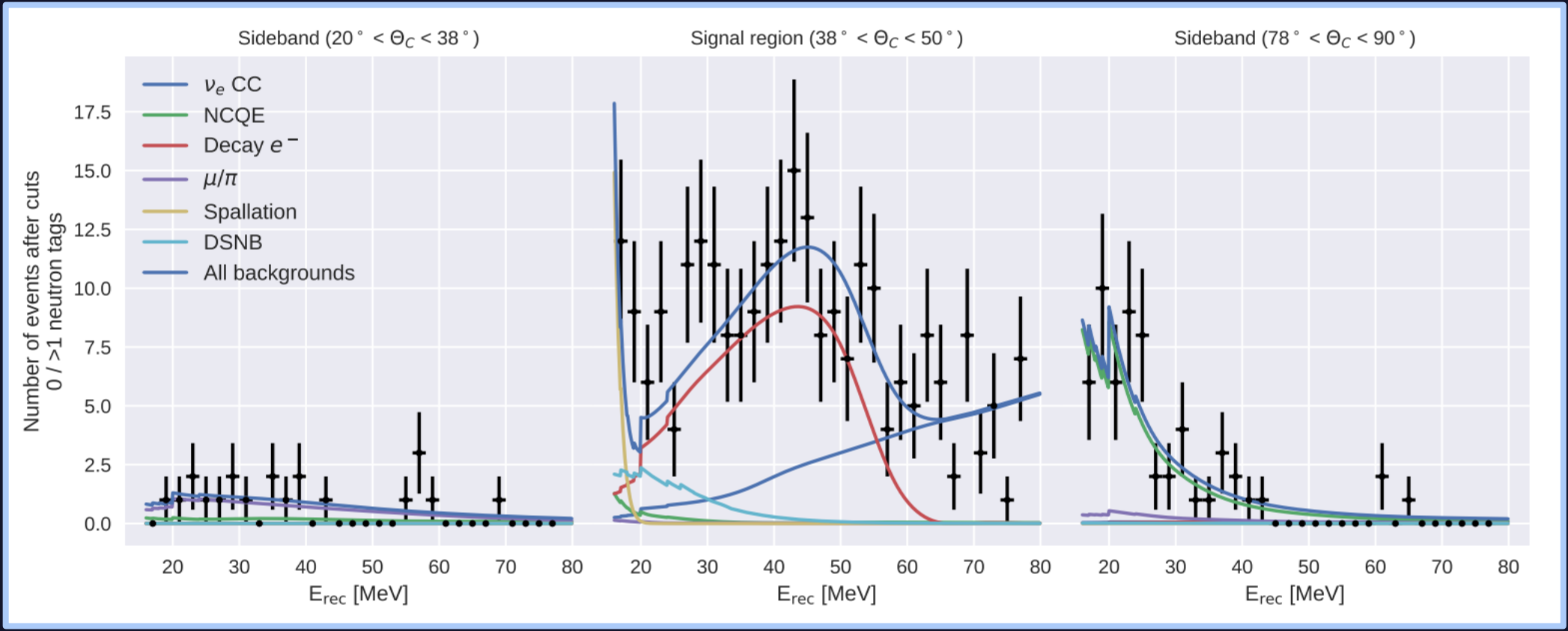

Super-Kamikande Collaboration, PRD 104 (2021) 122002

Hyper-Kamiokande Background

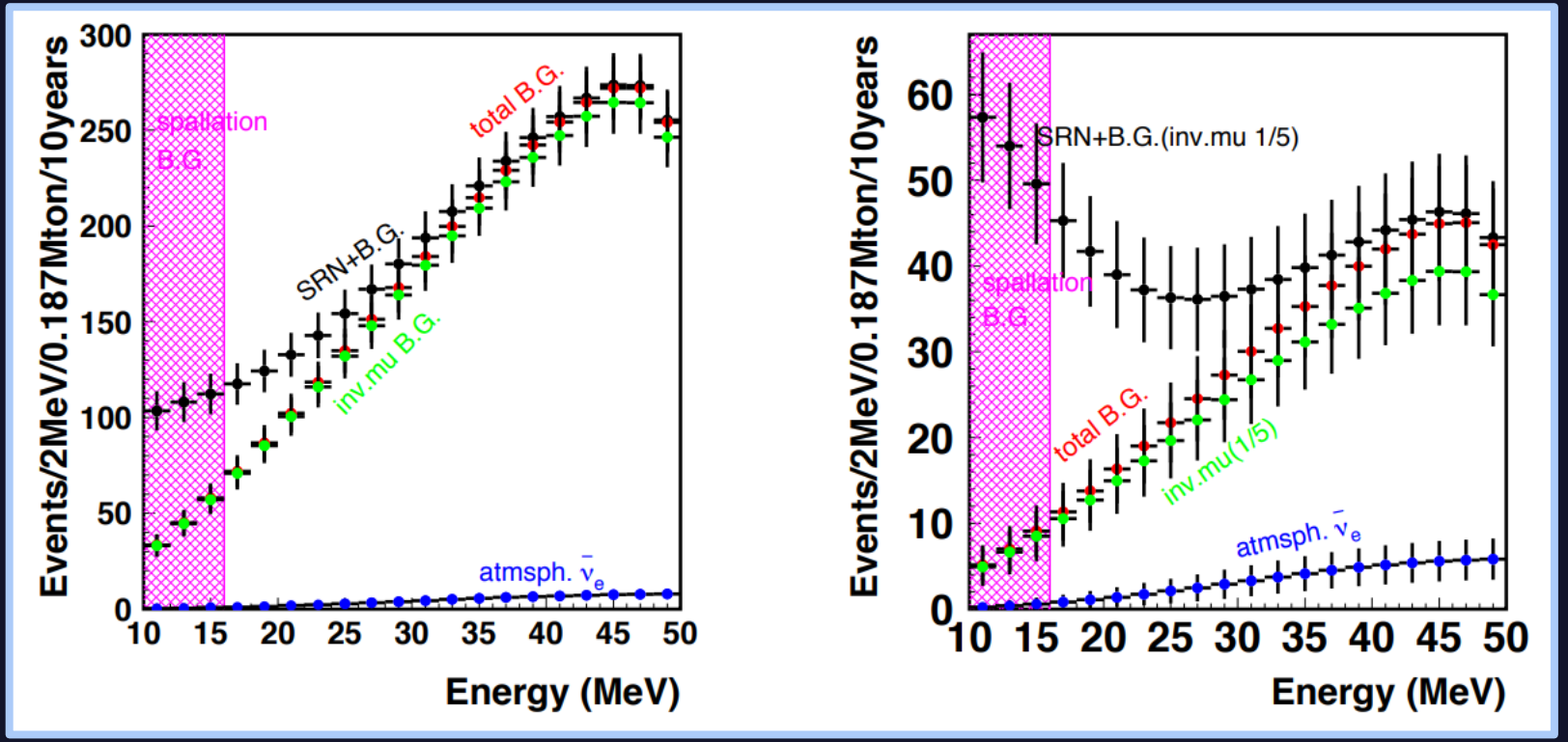

Hyper-Kamikande Collaboration [1805.04163]

Expected spectrum of SRN signals at Hyper-K with 10 years of lifetime without tagging neutrons. Left figure shows the case without tagging neutrons, assuming a signal selection efficiency of 90%. Neutron tagging were applied for right figure, with the tagging efficiency of 67% and the pre-gamma cut for invisible muon background reduction. The black dots show the sum of the signal and the total background, while the red shows the total background. Green and blue show background contributions from the invisible muon and ν_e components of atmospheric neutrinos.

ALPs from SN 1987A in Super-Kamiokande

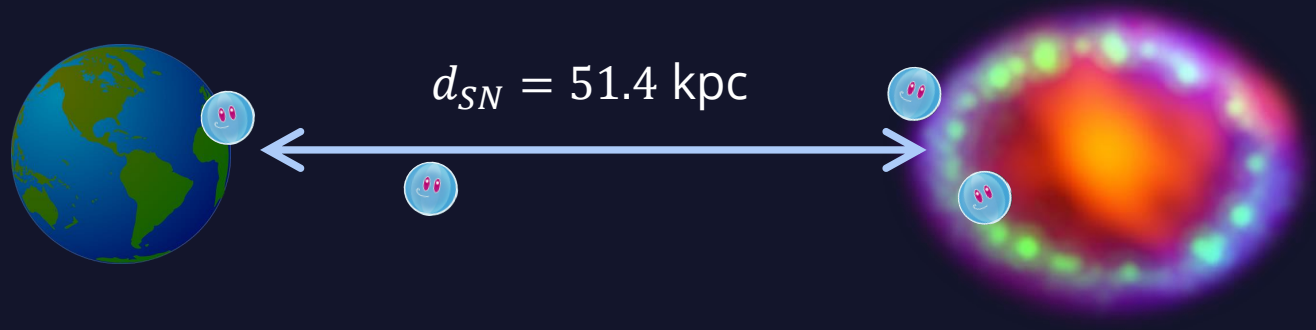

If they are massive enough, some of the ALPs produced in the SN 1987A could have been already detected by Super-Kamiokande.

The scenario that maximizes the signal corresponds to:

$$m_a \simeq 0.45 \text{ MeV}$$
$$g_{ap} \simeq 4 \times 10^{-5}$$

Taking into account the operation period of the first four SK phases (9 to 31 years after SN 1987A neutrinos) only ALPs with energies in the range $23.5 - 43.6$ MeV could have been observed.

But the statistical significance of the signal is only $Z \simeq 0.5$.

No constraints can be derived!

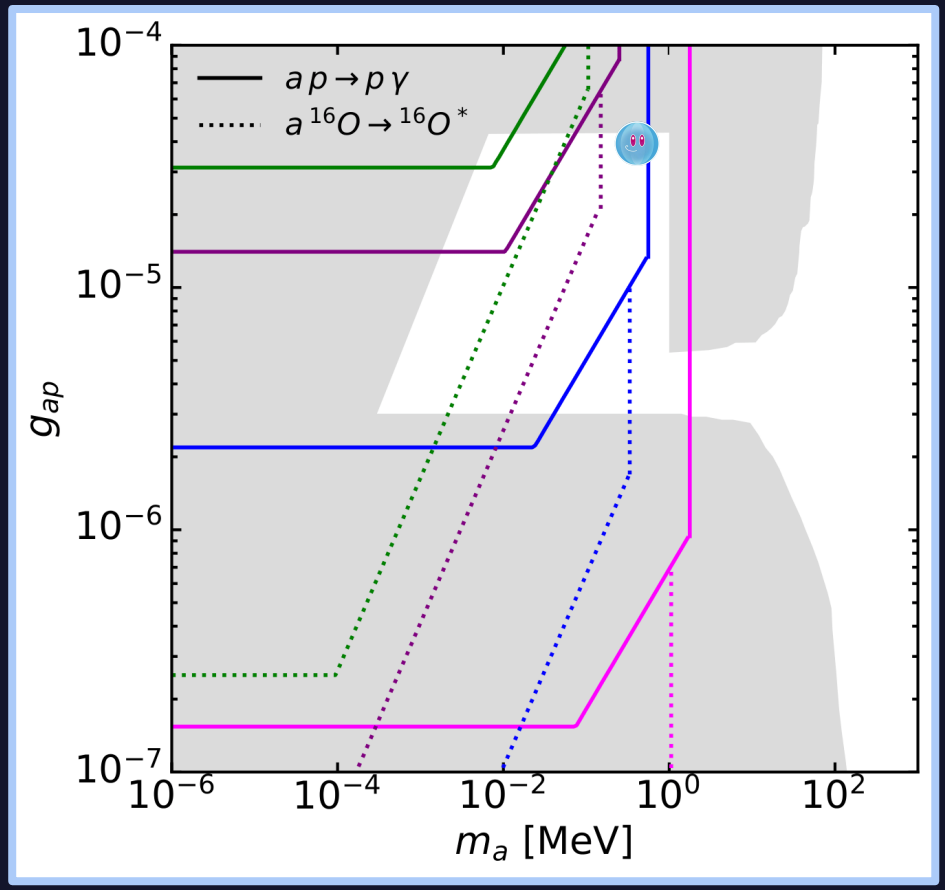

ALP detection via oxygen de-excitation

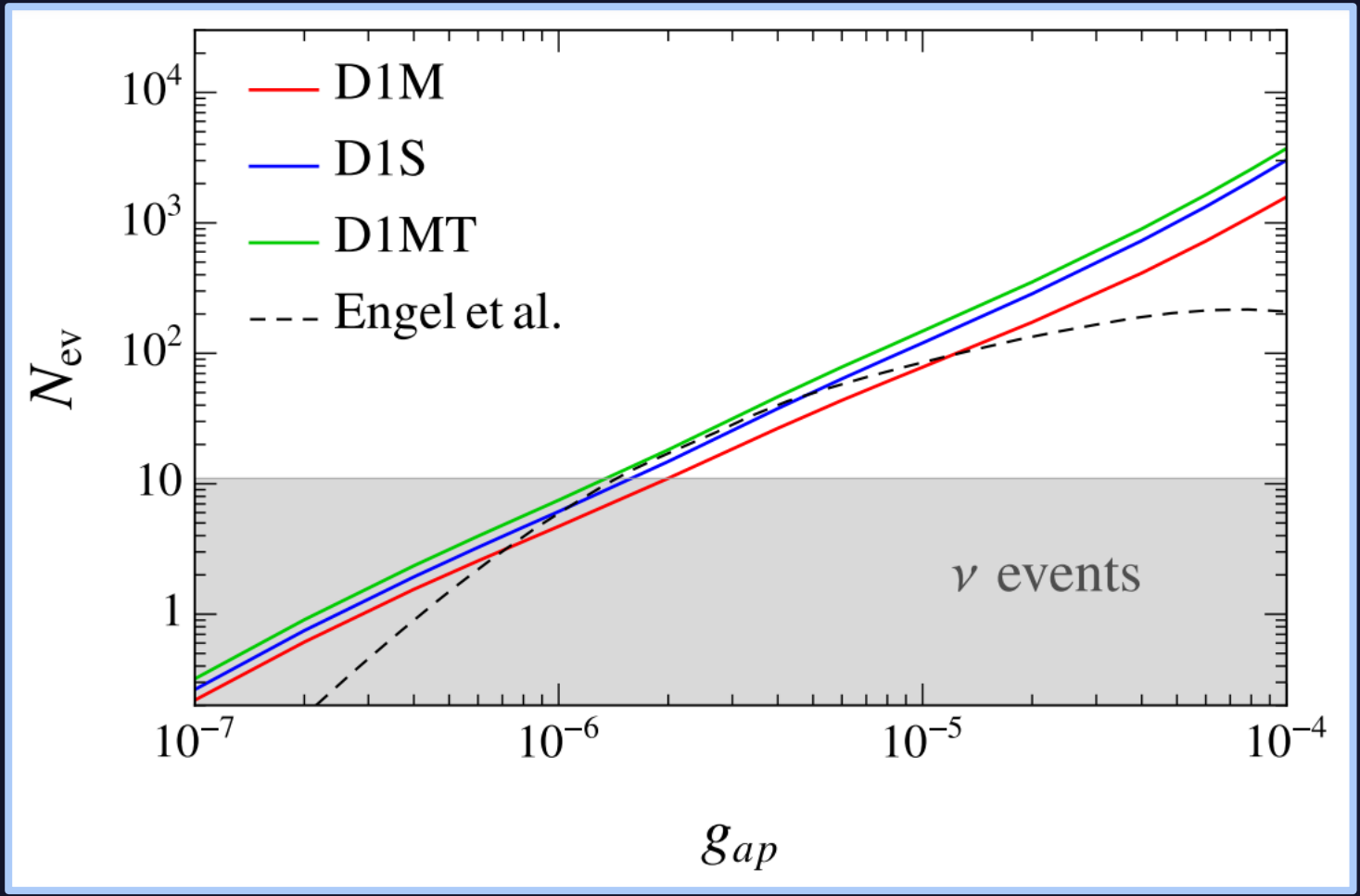

Predicted number of axion-induced events in **KII water Cherenkov detector** for the three different nucleon-nucleon interactions employed in the CRPA calculations as a function of the axion-proton coupling. The solid lines are obtained by exploiting the results for cross section introduced in this work and the spectra computed in *Lella et al., PRD 109 (2024) 2 023001*, while the dashed lines displays the number of events estimated in *Engel et al., PRL 65 (1990) 960*. The grey band defines the region where the number of events due to axions is submerged by neutrino events.

Carenza, Co', Giannotti, Lella, Lucente, Mirizzi, Rauscher, PRC 109 (2024) 1 015501